Agenzia nazionale per le nuove tecnologie,
l'energia e lo sviluppo economico sostenibile

MINISTERO DELLO SVILUPPO ECONOMICO

Ricerca di Sistema elettrico

Risultati relativi alla campagna sperimentale di medio termine sui fenomeni di erosione/corrosione da Litio liquido fluente nell'impianto Lifus 6

P. Favuzza, M. Cuzzani, V. Cuzzola, G. Fasano, A. Ventura

Report RdS/PAR2016/135

RISULTATI RELATIVI ALLA CAMPAGNA SPERIMENTALE DI MEDIO TERMINE SUI FENOMENI DI EROSIONE/CORROSIONE DA LITIO LIQUIDO FLUENTE NELL'IMPIANTO LIFUS 6

P. Favuzza, M. Cuzzani, V. Cuzzola, G. Fasano, A. Ventura (ENEA)

Settembre 2017

Report Ricerca di Sistema Elettrico

Accordo di Programma Ministero dello Sviluppo Economico - ENEA
Piano Annuale di Realizzazione 2016
Area: generazione di energia elettrica con basse emissioni di carbonio
Progetto: B.3.2 – Attività di Fisica della Fusione Complementari a ITER
Obiettivo: Progettazione e qualifica ingegneristica del target IFMIF – subtask b1. Forniture ed implementazioni comuni per progettazione, costruzione ed operazioni riguardanti gli impianti a litio ELTL e LiFUS 6 per attività sperimentali su corrosione/erosione, purificazione, termo idraulica e cavitazione per IFMIF
Responsabile del Progetto: A. Pizzuto, ENEA

Si ringrazia il dott. Stefano Caporali del *Consorzio Interuniversitario Nazionale Per La Scienza E Tecnologia Dei Materiali* per il supporto fornito nell'analisi chimica-metallografica dei provini utilizzati nel corso della campagna sperimentale.

Indice

Sommario

This report deals with the execution and the results of the last (2016-2017) erosion-corrosion test conducted in ENEA Brasimone centre with the Lifus 6 plant; this activity has been performed in the framework of the task LF03 of the IFMIF project.

This test entails to expose specimens made of Eurofer 97 and F82H, which are RAFM (Reduced Activation Ferritic Martensitic) steels, to the action of liquid Lithium flowing at 15 m/s and 330°C, in purity controlled conditions (Nitrogen concentration in Lithium ≤ 30 wppm). The test duration has been 2000 hours, as in the previous test, but, differently from this, here only half of the specimens (2 for each material) were fresh, while the other half (2 for each material) were already exposed, 'recycled' from the previous test: this way, these last 4 specimens experienced a total 4000 hours exposure to Lithium.

The outcome of the test shows the good resistance behavior of both Eurofer 97 and F82H to the adopted experimental conditions. Their maximum corrosion rate was about 0.29 µm/y, resulting largely lower than the limit set for the IFMIF Target backwall (1 µm/y) and around 1 order of magnitude lower than in a very similar experiment, performed in 2007 in Enea Brasimone, but employing a more contaminated Lithium.

Very few and small corrosion items were detected on the exposed surfaces and only a little Cr and W decrease was measured in the average surface compositions; the arise of a granulose appearance was evidenced, especially after longer exposure times. The internal structure of all the specimens was no way damaged. Difference between the 2 materials were trivial, with a bit higher Cr depletion from F82H surfaces at most.

The study of the steels resistance to the erosion-corrosion exerted by flowing Lithium has not been concluded with the test detailed in this report. In a close future experimentation, Lifus 6 plant will be employed again for this activity, allowing test durations longer than 4000 hours (they will be real 'long term' tests). Additionally, parametric studies will be performed, in which the concentration of Nitrogen in Lithium will be progressively raised till hundreds of wppm, to better quantify the effect of this parameter on the corrosion rate and in case highlight the existance of a threshold, above which the behavior of the exposed steels becomes all at once worse.

1 Introduzione

The evacuation of the large heat amount deposited by the Deuteron beam (10 MW) on the target footprint (0.01 m^2) of the IFMIF plant and the concurrent prevention of the Lithium boiling, dictate a linear speed of the flowing metal in the target section in the range of 10-20 m/s. Because of such a high value, not only corrosion, but the combined erosion-corrosion action exerted by the liquid Lithium is an issue of great importance among the many IFMIF validation activities (EVEDA), requiring to preventively assess the lifetime of the exposed target components, in particular the nozzle and the backplate. Apart from the components general thinning and the formation of wandering corrosion products in Lithium, local shape modifications due to erosion-corrosion could generate flow instabilities and lead to irregular Lithium film thickness or massive spills, causing in turn the beam trip off and the stop of the plant operation.

Limits of the erosion-corrosion rate have been specified in the IFMIF Comprehensive Design Report [1] as follows:

- 1 µm per year in the Target
- 50 µm over 30 years in the rest of loop

The topic of the erosion-corrosion is the subject of a specific IFMIF/EVEDA task, described by the LF03 Procurement Arrangement, assigned to Brasimone ENEA Techinical Unit. This task builds on the experience of a first exploratory run performed during 2007 with the LIFUS 3 plant in ENEA Brasimone Centre, in which both AISI 316 and Eurofer 97 specimens were put in contact for 1000 hours with liquid Lithium, flowing at 350°C and 16 m/s, but without a measured purity level [2].

In order to overcome this limit and to dispose of Lithium with controlled impurities amounts, so to comply with IFMIF operations, the LF03 PA indicated to realize a new, improved Lithium plant (Lifus 6), featuring also a purification system, consisting of:

- a Cold Trap, aimed at reducing Carbon and Oxygen concentration in Lithium below 10 wppm and Hydrogen one to about 60 wppm;
- an Hot Trap, aimed at reducing Nitrogen concentration in Lithium below 30 wppm;
- a Resistivity Meter, aimed at continuously monitoring the total impurity content in flowing Lithium;
- a sampling unit, allowing to take few grams of Lithium from the plant and to perform a specific batch chemical analysis on it, to precisely quantify the concentration of Nitrogen, the most corrosion affecting impurity.

The task entailed then to employ this new plant for the execution of 3 different erosion-corrosion tests. In all the 3 tests, 8 Reduced Activation Ferritic-Martensitic (RAFM) steels specimens, 4 made by Eurofer 97 and 4 by F82H, were exposed to liquid Lithium, flowing at ~ 15 m/s at 330°C and containing less than 30 wppm of solved Nitrogen. The first of these tests (*short term test*) was executed since mid-November 2015 to the beginning of 2016, lasting 1222 effective hours; the second one (*mid-term test*), involving 8 new (fresh) specimens, was instead executed since the 9th of March 2016 to the end of June 2016, covering an effective duration of exactly 2000 hours: the outcome of these 2 tests has been already reported in [3].

The last erosion-corrosion test, the '*long term*' one, is instead the main subject of this report. This test lasted again 2000 hours, but here only half of the specimens (2 for each material) were fresh, while the other 4 (2 for each material) were already exposed specimens, 'recycled' from the previous test: this way, these last 4 specimens experienced a total 4000 hours exposure to Li. The assessment of the damage/modifications induced on each specimen by the exposure to flowing Lithium has been based on the variation of its mass, its dimensions, its surface roughness, its morphology (both by optical and electronic microscopy) and its local chemical composition (by EDS), respect to the starting situation.

2 Descrizione delle attività svolte e risultati

2.1 Lifus 6 Test Section and specimens general properties

Before going into the details of the experiment and analyzing its results, a brief remind of the arranged setup and of the general properties of the investigated specimens.

Lifus 6 plant is the new plant realized in ENEA Brasimone centre starting from 2012 to execute the erosion-corrosion experimental tests; its design and functioning are reported in [4]. Here it is only sufficient to look at the configuration of Test Section of the plant (design shown in Figure 1), which is the part of the plant where the specimens are put in contact with the flowing liquid Lithium.

Lithium, which moves at ~ 30 L/min inside the plant, once entered the Test Section from the top, flows downwards through a thin duct, having an annulus section with just ½ mm span. The reduction of the pipe section produces the increase of the metal linear velocity in the duct up to about 15 m/s. The duct is realized by fixing, inside a pipe with an internal diameter of 21 mm (external dimension = 1" standard pipe), 8 specimens having the shape of hollow cylinders, with an outer diameter of 20 mm, an inner diameter (hole for the rod) of 10 mm and a height of 8 mm (see Figure 2). The specimens, perfectly aligned one above the other, expose therefore only their external cylindrical surface to the flowing Lithium.

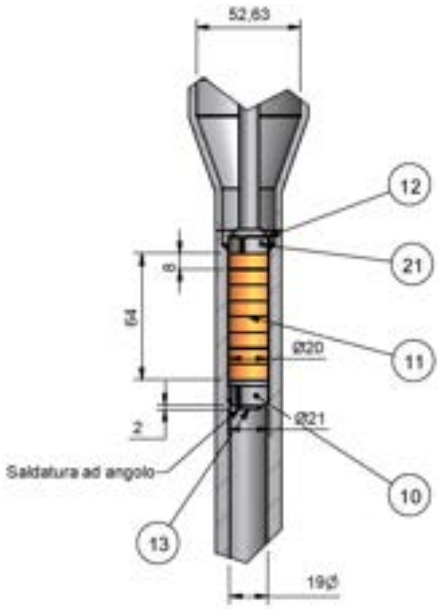

Figure 1: design of Lifus 6 Test Section, highlighting in yellow the specimens disposal. Physical dimensions are expressed in mm

For what concerns the investigated materials, they are both classified as Reduced Activation Ferritic-Martensitic (RAFM) steels, in that they are Iron alloys in which the presence of elements with long decay times due to activation by neutron irradiation (like Ni, Nb, Mo, Al…) must be as much as possible limited. The two materials have a very similar chemical composition, being characterized by about 8-9% by weight of Chromium (Cr) and little amounts of Manganese (Mn), Vanadium (V) and Tungsten (W): the only significant difference lies in the amount of W, which is ~ 2% in F82H, while it is ~ 1% in Eurofer 97. Precise chemical composition of the employed Eurofer 97 and F82H are reported respectively in Table 1 and Table 2, as determined by the producer of the alloys [5]. From a structural point of view, the two materials differ in the grain size, being in the order of 10 µm for the Eurofer 97 and about 50-100 µm for the F82H, as shown also in [3].

Figure 2: appearance of a fresh specimen, from the top

The specimens employed for the Lifus 6 experimental activities have been realized, in ENEA workshop, starting from large plates of the 2 materials. After assuming the right shape, the specimens have been subjected to a proper treatment of the surface exposed to Lithium, resulting in a roughness (Ra) around 0.3 μm. Each specimen has been then univocally marked with a numeric code (thin engraving) on the annular s

saarschmiede
Freiformschmiede
66330 Völklingen

GÜTEÜBERWACHUNG

WAZ-Nr.: 6427/1b
Anlage: 1

Kommission: Kunde: EFDA Marke: VIM+VAR 1.4914x3 , EUROFER 97-2

Chemische Zusammensetzung (Gew.-%) (Stückanalyse)

Schmelze-Nr.	C	Si	Mn	P	S	Ni	Cr	Mo	V	Ta	W	Ti	Cu	Nb	Al	N_2	B
Soll	0,090-0,120	< 0,050	0,20-0,60	< 0,005	< 0,005	< 0,01	8,50-9,50	< 0,005	0,15 0,25	0,10-0,14	1,00-1,20	< 0,02	< 0,01	< 0,005	< 0,01	0,015-0,045	< 0,002
993391	0,110	0,031	0,55	0,0010	0,001	0,013	8,95	0,005	0,202	0,120	1,06	0,001	0,005	0,005	0,009	0,022	0,0009

Co	As+Sn+Sb+Zr	O_2
< 0,01	< 0,05	< 0,01
0,004	0,009	0,0007

Erschmelzungsart / Melting Practice : VIM + VAR

saarschmiede
Güteüberwachung/Qualitätssicherung

Table 2. Chemical Composition(wt.%)

Heat No.	Roll No.		C	Si	Mn	P	S	Cu	Ni	Cr	Mo	V	Nb	B	T. N	Sol. Al	Co	Ti	Ta	W
9753		Ladle	0.09	0.08	0.1	0.003	0.001	0.01	0.02	7.89	0.003	0.19	0.0002	0.0002	0.006	0.001	0.003	0.004	0.02	1.99
9753	KG819-2 15t ingot top	check	0.09	0.07	0.1	0.003	0.001	0.01	0.02	7.87	0.003	0.19	0.0002	0.0002	0.006	0.001	0.003	0.004	0.04	1.98
9753	KG819-1 15t ingot middle	check	0.09	0.07	0.1	0.003	0.001	0.01	0.02	7.87	0.003	0.19	0.0002	0.0002	0.007	0.001	0.003	0.004	0.03	1.98
9753	KG820-2 25t ingot middle	check	0.09	0.07	0.1	0.003	0.001	0.01	0.02	7.84	0.003	0.19	0.0002	0.0002	0.007	0.001	0.003	0.004	0.04	1.98
9753	KG820-1 25t ingot bottom	check	0.09	0.07	0.1	0.003	0.001	0.01	0.02	7.82	0.003	0.19	0.0002	0.0002	0.007	0.001	0.002	0.004	0.04	1.98

Table 3. Tensile Properties

Heat No.	Roll No.	Ingot position	RT			500℃		
			YS(MPa)	UTS(MPa)	El.(%)	YS(MPa)	UTS(MPa)	El.(%)
9753	KG819-1	top	553	681	26	438	474	20

2.2 Starting specimens characterization

It is of course necessary to characterize each specimen before starting the test, in order to compare it to itself at the end of the test. The starting physical parameters of the 8 employed specimens are reported in Table 3.

Specimens #7, #8, #28 and #29 (gray background in the table) had been already employed in the previous (medium-term) test, therefore at the moment of being inserted in the Test Section they had already experienced 2000 hours of exposure to Lithium. Values reported for them in Table 4 refer anyway not to the condition just before the start of the last experimental test, but to their fresh condition, i.e. before also the previous 2000 hours. The comparison with these original values permit to evaluate the overall effect on them of 4000 hours exposure to Lithium.[1]

Table 3: starting physical parameters of the specimens employed in the long term test

Material	Sample ID	Height* [mm]	External Diameter[1] [mm]	Mass** [g]
Eurofer 97	7	8.022	19.996	14.74200
Eurofer 97	8	8.017	19.997	14.73279
Eurofer 97	12	8.019	20.002	14.74926
Eurofer 97	13	8.020	20.002	14.74780
F82H	28	8.035	20.001	14.85061
F82H	29	8.031	20.000	14.84441
F82H	32	8.032	19.997	14.84045
F82H	34	8.034	20.001	14.85056

* All the specimens are characterized by a parallelism error = 0.002 mm and a diameter ovalization = 0.001 mm

** The Std Dev of the measurement is ≤ 0.02 mg, as declared by the supplier of the employed balance.

Additionally, one fresh specimen for each material (not devoted to the test) has been subjected to the determination of the surface roughness profile, the optical microscope/stereoscope visual inspection and the scanning electron microscope observation (SEM) and the verification of the chemical composition (EDS analysis), as representative of all the specimens of the same material. The results of these investigations, performed in ENEA Brasimone centre, are illustrated by Figures 3 to 5, for Eurofer 97, and Figures 6 to 8, for F82H. It must be underlined that the EDS analysis doesn't provide an extremely accurate composition, in that each element concentrations is commonly affected by an error of about ± 0.5 at.%, the error varying with the specific element; moreover, low mass element (< Fluorine), cannot be correctly quantified. The EDS analyses anyway confirmed that the specimens materials compositions matched the ones in Table 2 and 3.

[1] Mass variation of Specimens #7, #8, #28 and #29 after the first 2000 hours of exposure to flowing liquid Lithium were reported in [3].

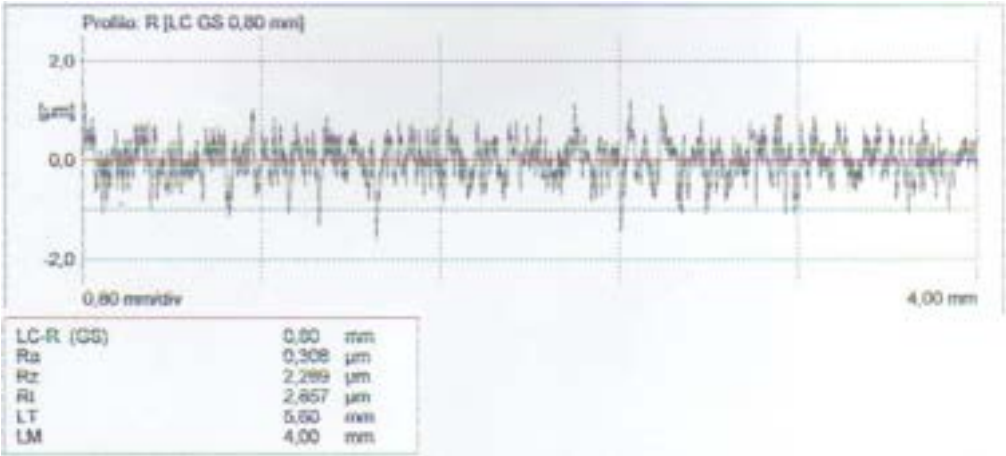

Figure 3: roughness profile of the external surface of a representative Eurofer 97 specimen

Figure 4: stereoscope image of a representative Eurofer 97 specimen: curved external surface, viewed from the top. The surface is in good shape.

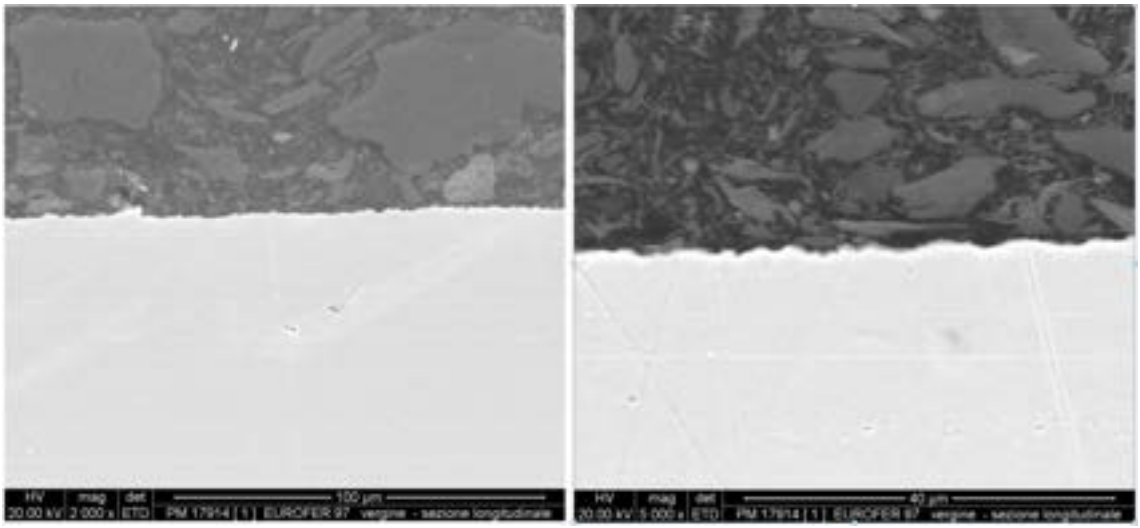

Figure 5: SEM images (secondary electrons) of a representative Eurofer 97 specimen: longitudinal sections. The surface is in good shape (dark region in the top half is due to graphite, where the specimen is mounted in).

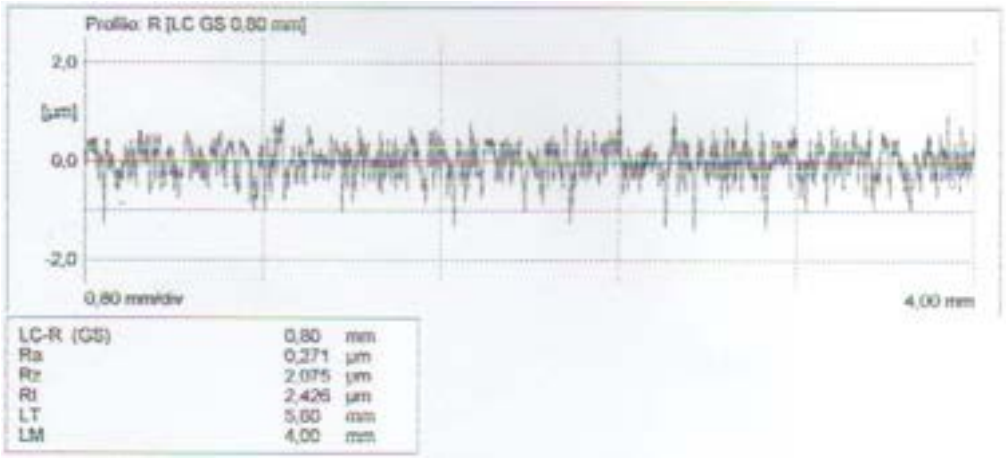

Figure 6: roughness profile of the external surface of a representative F82H specimen.

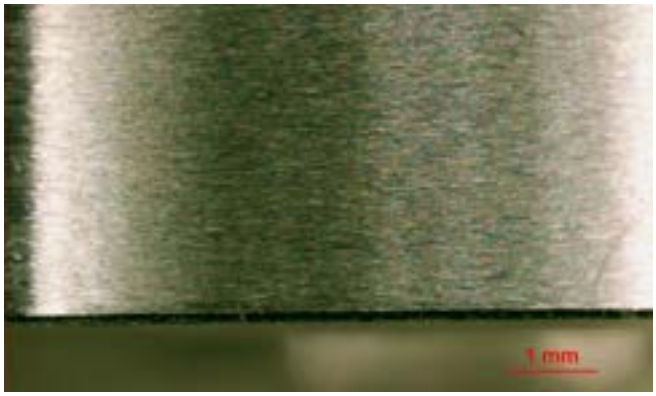

Figure 7: stereoscope image of a representative F82H specimen: curved external surface, viewed from the top. The surface is in good shape.

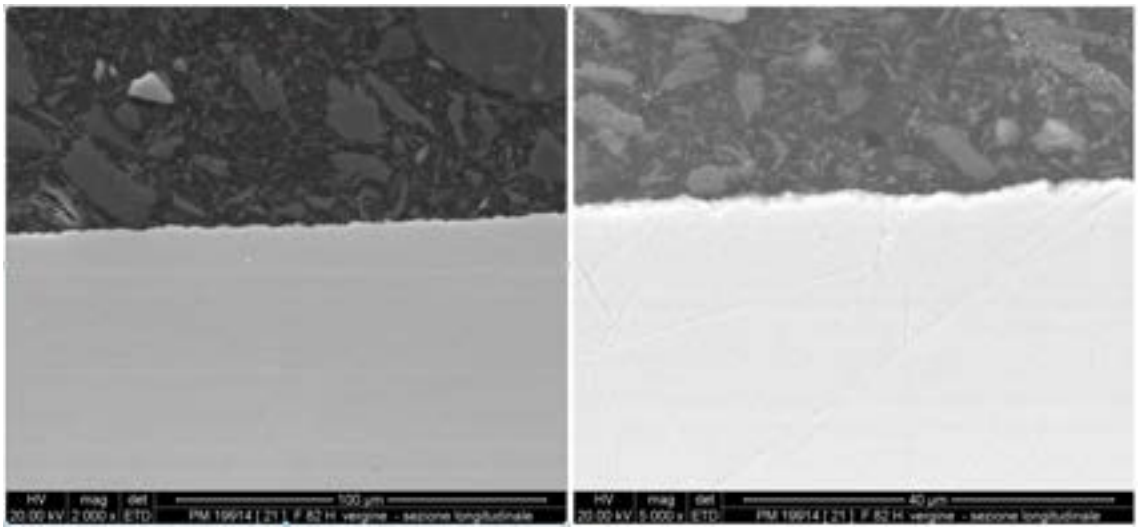

Figure 8: SEM images (secondary electrons) of a representative F82H specimen: longitudinal sections. The surface is in good shape (dark region in the top half is due to graphite, where the specimen is mounted in).

2.3 Erosion-corrosion test execution

The 8 specimens submitted to the erosion-corrosion test have been inserted inside Lifus 6 Test Section according to the scheme shown in Figure 9 (left). It is important to take note of the exact sequence of the specimens inside the plant, not only to overcome the possible erasing of the identification code at the end of the test, but also to verify if there could be a different experimental answer from the specimens of a same material depending on their different location. Some Lithium flow turbulence in fact could occur at the entrance of the Test Section duct, therefore the actual flow conditions could slightly change along the length of the duct, determining a not identical erosion action. For the same reason, the sequence of the two materials in the Test Section is alternate, to realize for them the most similar experimental conditions. Specimens recycled from the previous test have been located in the central positions of the Test Section, the same they occupied also previously: they are clearly identifiable, since they appear less glossy than the other 4, fresh, ones (Figure 9, right).

Figure 9: specimens arrangement inside Lifus 6 Test Section. Left: scheme with the real sequence of specimens; right: appearance of the specimens mounted on the rod to be inserted in the Test Section

For what concerns the Nitrogen concentration in Lithium, it was quantified just before the start of the test through the offline chemical analysis [6-7] of a sample of Lithium taken from the plant, as 14.1 ± 2.1 wppm, largely complying with the test requirement (≤ 30 wppm). The test started around midday of the 30th of August, 2016 and terminated in the morning of the 22nd of November, lasting 2000 effective hours. It was properly accomplished for what concerns the condition of Lithium in contact with the investigated specimens, in that its flow rate was registered for the entire duration around 29 L/min, with usual oscillation not exceeding ± 2 L/min (see Figure 10). Only in a few and isolated cases negative spikes are seen, generally due to momentary voltage drops ascribable to the external electrical grid and affecting the main electromagnetic pump functioning, or, as in the case at ~ 840 and ~ 1200 hours, due to the Cold Trap Aircooler electrical malfunctioning (finally solved by changing the Aircooler engine). Anyway, after these snags, the pump rescued quickly its working setting.

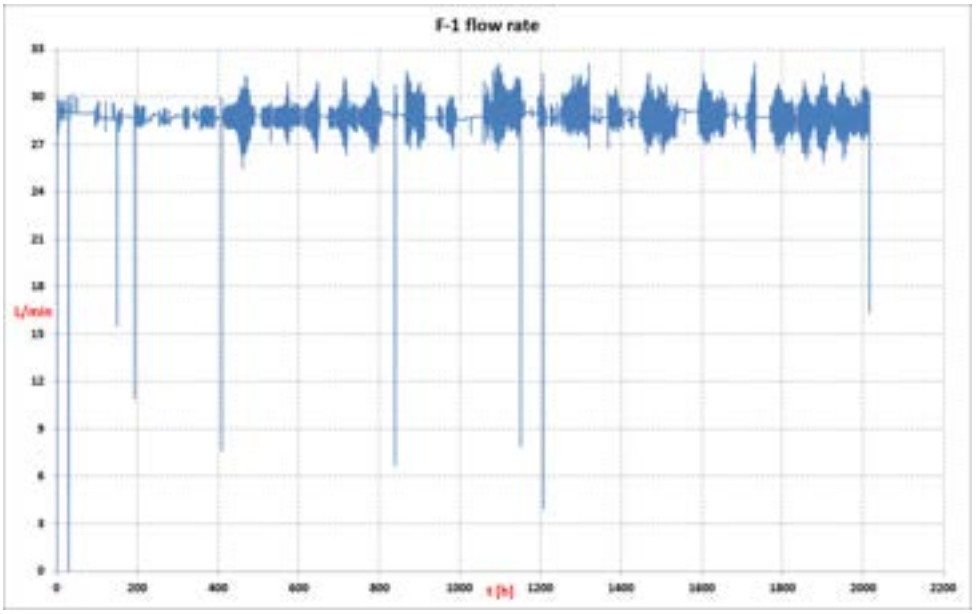

Figure 10: trend of the Li flow rate inside main Lifus 6 loop (and Test Section) during the whole experimental test.

Similarly, also the registered temperature of Lithium in the Test Section was essentially constant, with only isolated fluctuactions of few degrees around 330°C, the value set for the test (see Figure 11). Negative spikes are related to the same phenomena originating the spikes in Figure 10 at the same time coordinate.

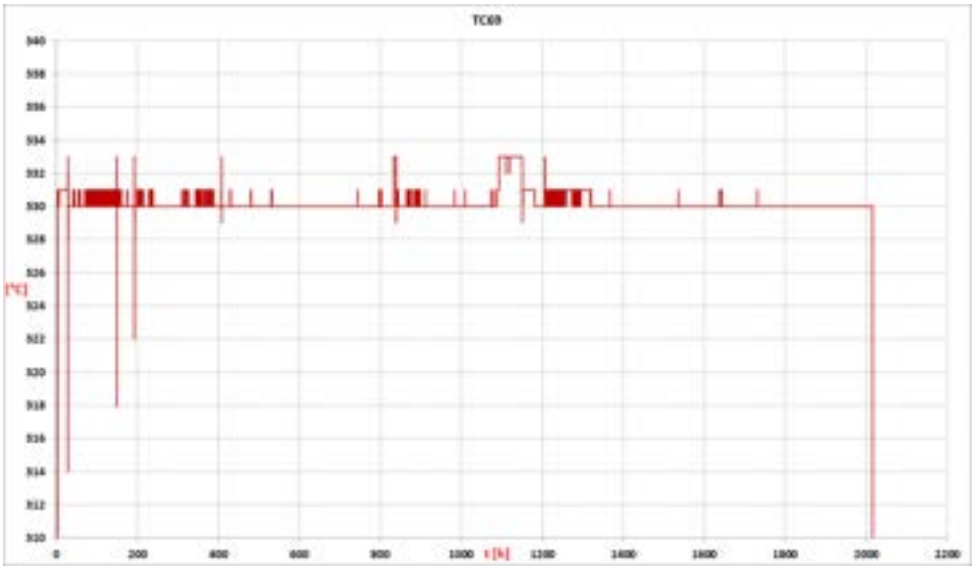

Figure 11: trend of the registered temperature of Lithium in the Test Section during the whole experimental test

At the end of the test a new offline analysis of Nitrogen concentration in Lifus 6 Lithium was executed, by sampling a little amount of the metal from the plant. Nitrogen concentration result was: 31.0 ± 4.2 wppm. This value is a bit higher than the starting one, however it'still adequate for the erosion-corrosion test requirement; it is moreover reasonable to think that Nitrogen concentration was confined within the starting and the final values during the entire test, validating therefore the test itself.

Once drained the plant and cooled to room temperature, it was possible to open the Test Section and remove, from the top, the rod holding the specimens. The operation was performed while flowing Argon from the bottom of the section, to exclude air (lighter than Argon) entering the plant.

2.4 Post-test analysis of the specimens

2.4.1 Mass variation and generalized corrosion rate

Once removed from the rod, the 8 specimens were thoroughly washed with water to remove sticking Lithium residues. Then they were submitted to a more pronounced cleaning treatment, by letting them in boiling water for 45 minutes. After drying, they were weighed.

Table 4 reports the values of their mass variations calculated respect to the corresponding values before the test (Table 3). From the knowledge of the mass variation of each specimen, the exact value of the surface exposed to flowing Lithium (simply given by the product: $\pi * d_e * h$, where d_e and h are respectively the external diameter and the height of the specimen, as reported in Table 3), the densities of the specimens materials (7.9 g/cm^3) and the total time of the test (2000 or 4000 hours), it is moreover possible to estimate the corrosion rate [µm/y] of the specimens in the applied experimental conditions. This quantity of course provides only a partial indication of the outcome of the test, in that it does not consider the local corrosion phenomena as well as the possibility of inclusion of external elements in the material lattice, giving instead an average answer, in quantitative terms, of the surface behaviour. It should therefore be better indicate as 'generalized' corrosion rate, as if the specimen material was simply homogeneously dissolved by the flowing metal. Calculated corrosion rates for the 8 investigated specimens are reported in Table 4 too.

Table 4: mass variations and generalized corrosion rates. Gray background specimens are those already employed in the previous test: their parameters are evaluated considering the overall exposure time (4000 hours).

Material	Sample ID	Mass variation [mg]	Corrosion rate [µm/y]
Eurofer 97	7	- 0.39 ± 0.03*	0.21 ± 0.02
Eurofer 97	8	- 0.31 ± 0.03	0.17 ± 0.02
Eurofer 97	12	- 0.15 ± 0.03	0.17 ± 0.03
Eurofer 97	13	- 0.20 ± 0.03	0.22 ± 0.03
F82H	28	- 0.23 ± 0.03	0.13 ± 0.02
F82H	29	- 0.52 ± 0.03	0.29 ± 0.02
F82H	32	- 0.05 ± 0.03	0.05 ± 0.03
F82H	34	- 0.01 ± 0.03	< 0.04

* ± 0.03 mg is the Standard Deviation of the weighing process

All the specimens are characterized by a very small weight loss, in absolute terms. For the specimens which had been already exposed to Lithium also in the previous erosion-corrosion test, the weight loss is surely higher, but, considering the double exposure time, the resulting corrosion rate is aligned to the one calculated for the fresh ones. This is particularly true for Eurofer 97, while for F82H the 'recycled' specimens result a bit more attacked than the fresh ones. Actually, if we consider also the corrosion rate results of the previous (mid-term) test, already reported in [3], it can be inferred that these second 2000 hours produced, on the average, a bit larger alteration on the specimens, compared to the first 2000 ones.

This could be due to a slightly higher contamination from non metallic elements other than nitrogen during the last test (they cannot be quantified), or, for what concerns the 'recycled specimens', to a starting test condition which didn't correspond exactly to the fresh test condition (the 'recycled specimens' had been extracted, cleaned and weighed at the end of the previous test, and this operation could have somehow modified the surface structure created in response to the first exposure to Lithium; in this regard, a 2000+2000 hours test could not correspond exactly to a 4000 hours test). In any case the differences are rather small, and, mostly, the largest measured corrosion rate is < 0.3 µm/y for the 4000 hours specimens, while is ~ 0.22 µm/y for the 2000 hours specimens: values significantly smaller than IFMIF requirement (< 1 µm/y).

2.4.2 Diameter and height variations

To complete the measurement of the physical parameters of the specimens, also the external diameter and the height of each of them have been precisely determined. The variations, evaluated respect to the corresponding values of the fresh specimens before the test (Table 3), result for all of them ≤ measure uncertainty (0.002 mm), therefore it can be concluded that no real variation took place. This evidence reflects what expected on the basis of the already reported mass variations.

2.4.3 Optical stereoscope inspection

Figure 12 shows 2 different views of the external surface of specimen #12 (Eurofer 97, 2000 hours total exposure, exit of the Test Section) after the test. The surface is smooth and regular. Compared with the appearance of a fresh Eurofer 97 specimen (Fig. 4), no difference is evident, a part from (perhaps) some very light stripes going along the specimen height.

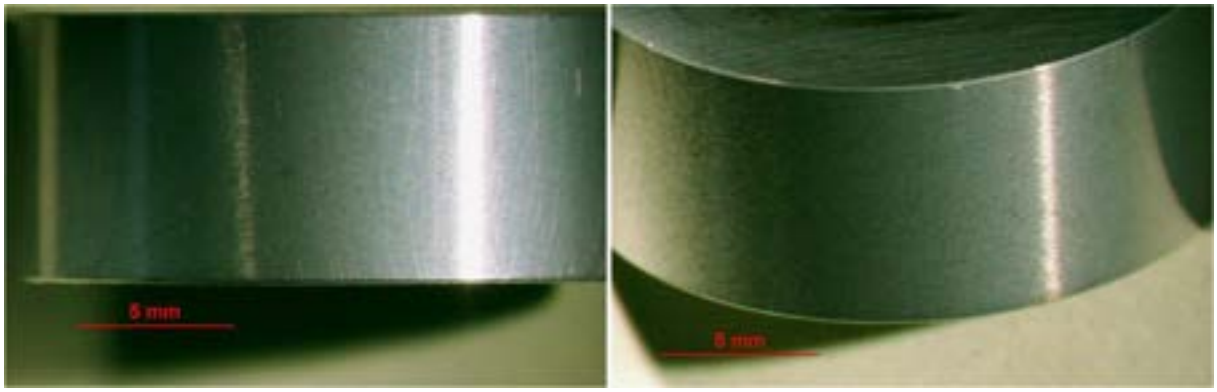

Figure 12: optical stereoscope inspection of the surface of tested specimen #12 (Eurofer 97, 2000 hours).

Figure 13 shows instead 2 different views of the external surface of specimen #7 (Eurofer 97 again, but 4000 hours total exposure, inner of the Test Section). The surface is smooth and regular; some very light stripes going along the specimen height can be noted again, which don't appear, however, more pronounced than for the previous specimen.

Figure 14 shows 2 different views of the external surface of specimen #34 (F82H, 2000 hours total exposure, entering of the Test Section) after the test. The surface is smooth and regular. Compared with the appearance of a fresh F82H specimen (Fig. 7), no difference is evident, nor even the light stripes seen in the previous specimens.

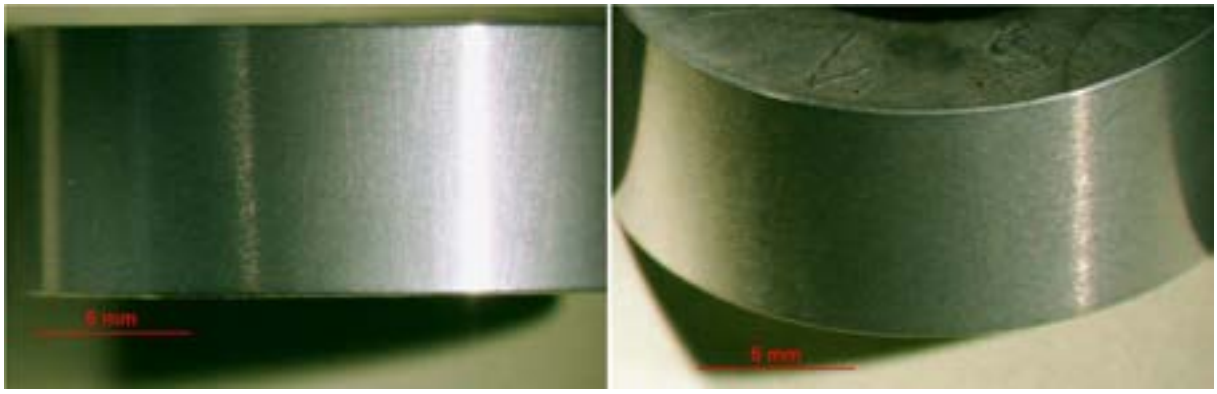

Figure 13: optical stereoscope inspection of the surface of tested specimen #7 (Eurofer 97, 4000 hours).

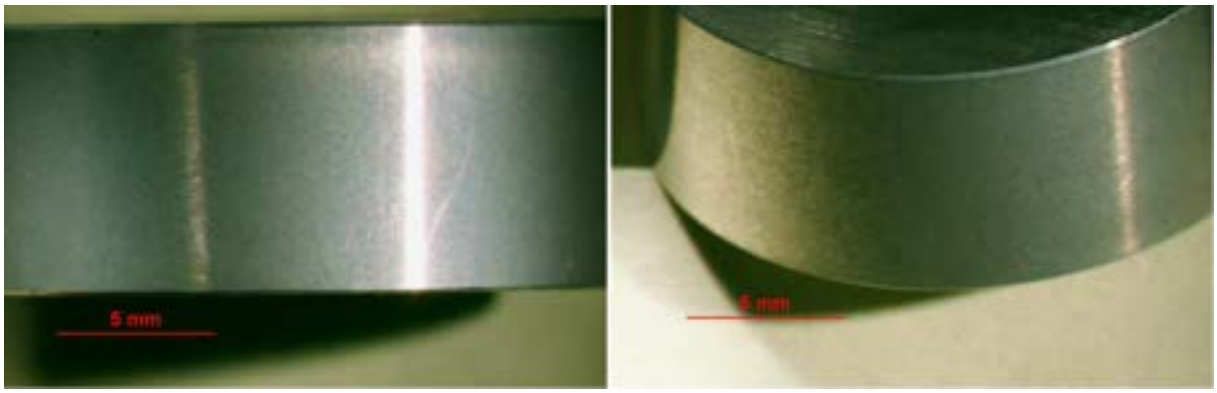

Figure 14: optical stereoscope inspection of the surface of tested specimen #34 (F82H, 2000 hours).

Figure 15 finally shows 2 different views of the external surface of specimen #28 (F82H again, but 4000 hours total exposure, inner of the Test Section). The surface is smooth and regular; some very light stripes going along the specimen height can be noted, a little more pronounced than in the two previous Eurofer 97 specimens.

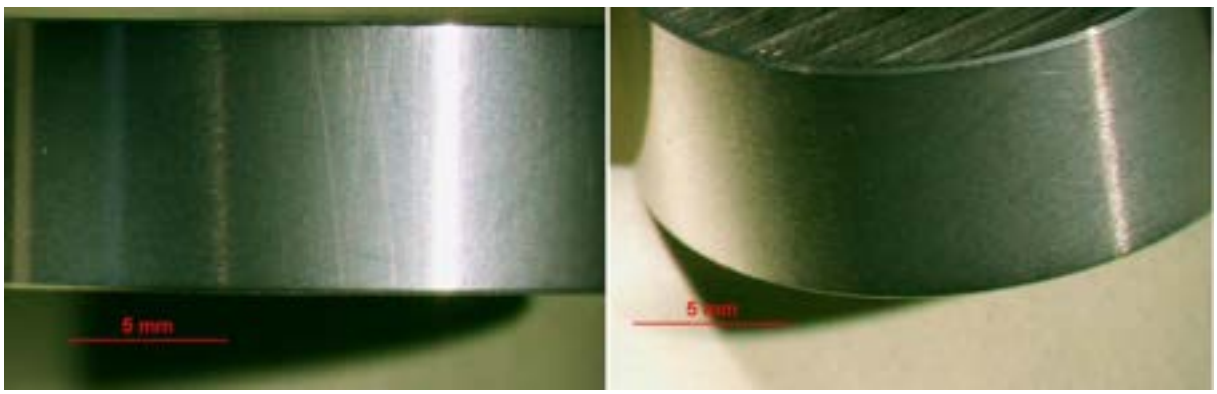

Figure 15: optical stereoscope inspection of the surface of tested specimen #28 (F82H, 4000 hours).

On the whole, the appearance of the specimens after the test confirms the rather small damage provoked on them by the flowing Lithium. Some doubt remains about the nature of the light stripes visible on the left side of each of the previous figures, whether they result from just visual artifacts or they correspond to a real physical situation: in this case, they could indicate that the mass lost by the specimens is to some extent due also to an erosive effect exerted by the flow of Lithium, since a purely chemical dissolution would have been more isotropic on the specimen surface and would not have marked a specific attack direction.

2.4.4 Roughness profile of the specimens

In order to evaluate possible changes in specimens roughness, it is necessary to make reference to Figures 3 and 6, which report the roughness profiles respectively for a representative Eurofer 97 fresh specimen and for a representative F82H fresh specimen (the roughness profile was not specifically determined for each employed specimen before the test, and the variations must be intended as qualitative) and the following measured parameters: Ra = 0.308, Rz = 2.289 and Rt = 2.857 µm for the Eurofer 97, and Ra = 0.271, Rz= 2.075 and Rt = 2.426 µm for the F82H.

For what concerns the 2 Euforer 97 specimens tested for 2000 hours, the shape of their profiles are apparently not different from the reference one, but the three measured parameters result for both a bit smaller, with a Ra value equal to 0.240 (#12) and 0.243 (#13). Looking at the 2 Eurofer 97 specimens subjected to a total 4000 hours exposure to Lithium, the parameters are all a bit smaller again, with a Ra value equal to 0.295 (#7) and 0.241 (#8); the differences of the roughness parameters respect to 2000 hours specimen are anyway statistically not meaningful.

For what concerns the 2 F82H specimens tested for 2000 hours in Lithium, the measured roughness parameters are all a bit smaller than reference, with a Ra value equal to 0.246 (#32) and 0.237 (#34). The F82H specimens tested for 4000 hours are similarly characterized by a small decrease of all the parameters with a Ra value equal to 0.240 (#28) and 0.270 (#29). Again, no decreasing trend with the exposure time is evident in these parameters.

Reasoning in terms of average behaviour (in view also of the unicity of each one specimen), it can be said that no difference has been highlighted in the variation of the roughness profile depending on the different specimen material, nor depending on the single or the double exposure to Lithium. Ra, Rt and Rz decreased a little for all the 8 specimens and this indicates the roughness profile was made a bit smoother by the flowing Lithium: the material removal, both by chemical dissolution or mechanical action (erosion), took place preferentially on the more protruding parts of the specimen surface.

2.4.5 SEM-EDS inspections of the specimens surfaces and sections

All these inspections were not executed in ENEA Brasimone centre, but in Firenze, by the INSTM Consortium (National Interuniversity Consortium of Materials Science and Technology), with whom a collaboration had been activated.

Each specimen, once received from ENEA, was cut through a cropper (Remet MT micro) in two pieces: the first one was employed for the morphological and chemical analysis of the surface; the second one, after insertion into a resin and lapping, was employed for the section investigation (Figure 16). Both fragments, after the cut, were washed with demineralized water and dipped into acetone in a ultrasonic bath for 3 minutes; after being rinsed again with water and then acetone, they were dried at room temperature. The fragment of specimen employed for the section observation was inserted into a phenolic resin, then polished with abrasive papers (from 180 to 2500 grit) and diamond pastes (9, 6 and 3 µm, Metadi suspension, Buehler); finally, to improve the quality of the SEM observation, the conductivity of the specimen was enhanced by applying a thin graphite layer, through an evaporation under vacuum process.

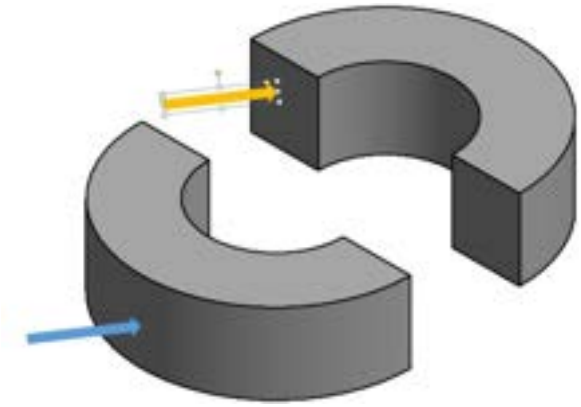

Figure 16: scheme of the specimen cut in 2 parts. Yellow arrow indicates the investigated section area; blue one indicates the investigated external surface area.

The investigations were performed employing an Hitachi 2300 electron microscope (SEM) equipped with an X-ray spectrometer with energy dispersion (EDS) controlled by the Noran System Six 3600 software. It must be emphasized that the EDS analysis is intrinsically affected by un uncertainty of ~ 0.5% in the atomic concentration of each element.

Next subsections report the results of the SEM-EDS investigations of the 8 tested specimens. Together with them, are presented also the results of the same investigations performed on specimen #10 and #31, respectively a fresh (unexposed) Eurofer 97 specimen and a fresh F82H specimen. These results, already reported in [3], are presented here again in order to permit an easier comparison and highlight possible chemical/morphological alterations produced by the erosion-corrosion test.

2.4.5.1 Eurofer 97: specimen #10 (unexposed)

First of all, let's consider the Eurofer 97 specimen not submitted to the erosion-corrosion action by the flowing liquid Lithium (fresh specimens, #10).

Figure 17 shows, at different magnitudes (400 X and 2000 X), the surface of a representative region of this specimen: the scrapes of the mechanical manufacturing are clearly visible.

Figure 18 reports the EDS spectrum of this surface; Table 5 summarizes the values of the related compositional analysis (average of a ~ 800 x 1000 μm^2 area).

Figure 19 shows, on the left, a SEM representative image of specimen #10 section, with the red Chromium concentration profile overlapped, as determined by the EDS analysis; the dark region is due to the supporting resin. On the right side of Figure 19 is instead reported a graph showing the profiles of both Chromium and Iron elements, where y-axis is the weight % concentration, while x-axis indicates the distance from the surface (the surface position is on the right boundary of the graph; x = 0 corresponds instead to the starting point of the yellow arrow). Many equidistant points have been considered for the EDS analysis, in the arrow direction, from a starting a depth of ~ 35 µm below the surface. The profiles have been constructed by joining the calculated points with straight lines. The absolute values of both Cr and Fe are probably a bit higher than the real one, because other minority elements have been excluded from the calculation, hence the software calculates the Cr and Fe concentration values in a way their sum is 100%: what is important is the qualitative trend of the profiles.

From the observation of Figure 19, it is possible to note that the internal specimen structure is in good condition, with only some sign due to the cut and preparation of the sample, but no erosion-corrosion damage: this is of course what expected, since specimen #10 is an unexposed specimen. The concentration profiles indicate a substantial constancy of values; the minimal value of Cr concentration at the highest value of x is not phisically sure, because this measurement point was too close to the specimen border.

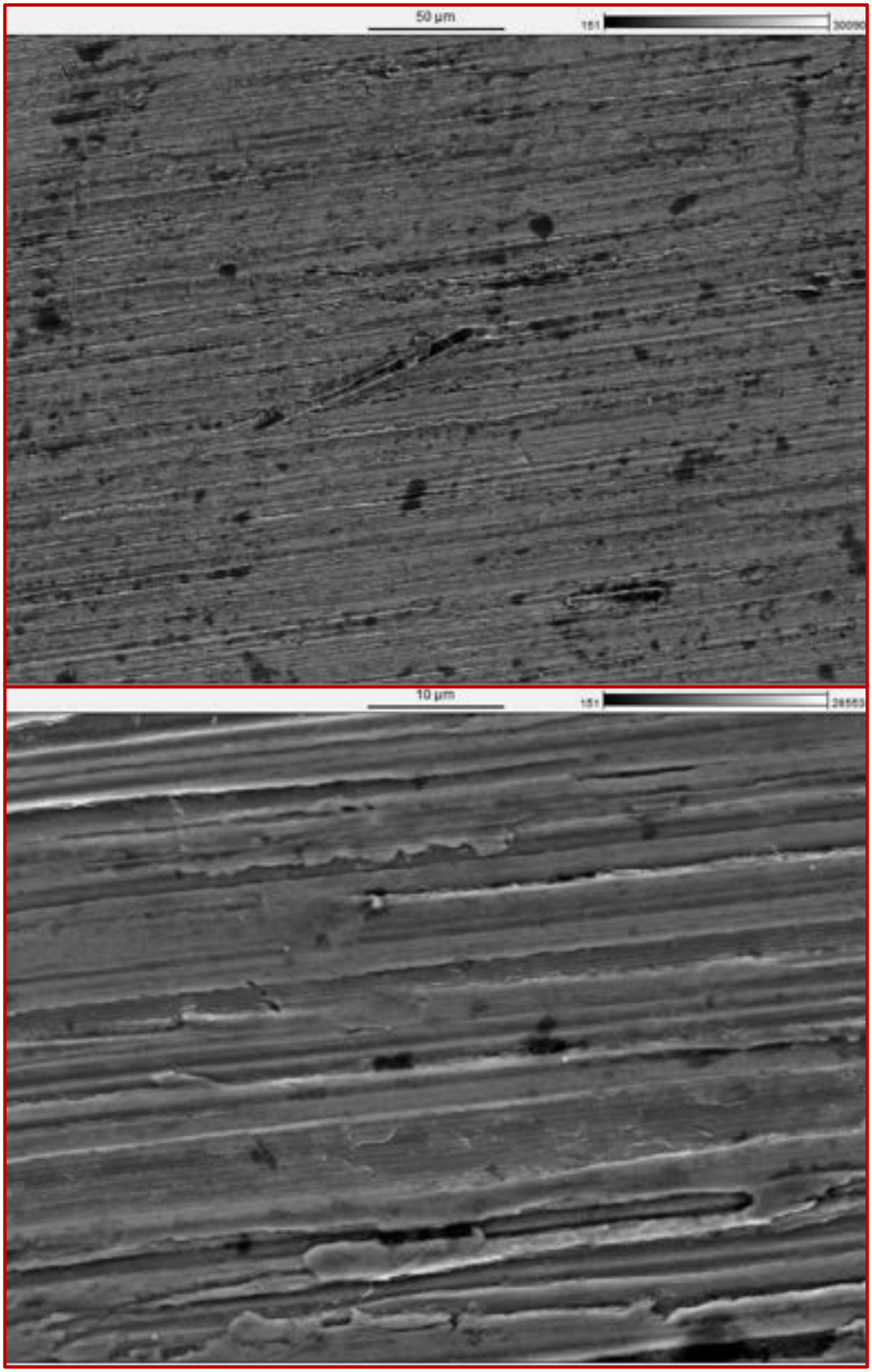

Figure 17: SEM images of specimen #10 surface (secondary electrons) at magnitude 400 X (top) and 2000 X (bottom). Scale bars above the images.

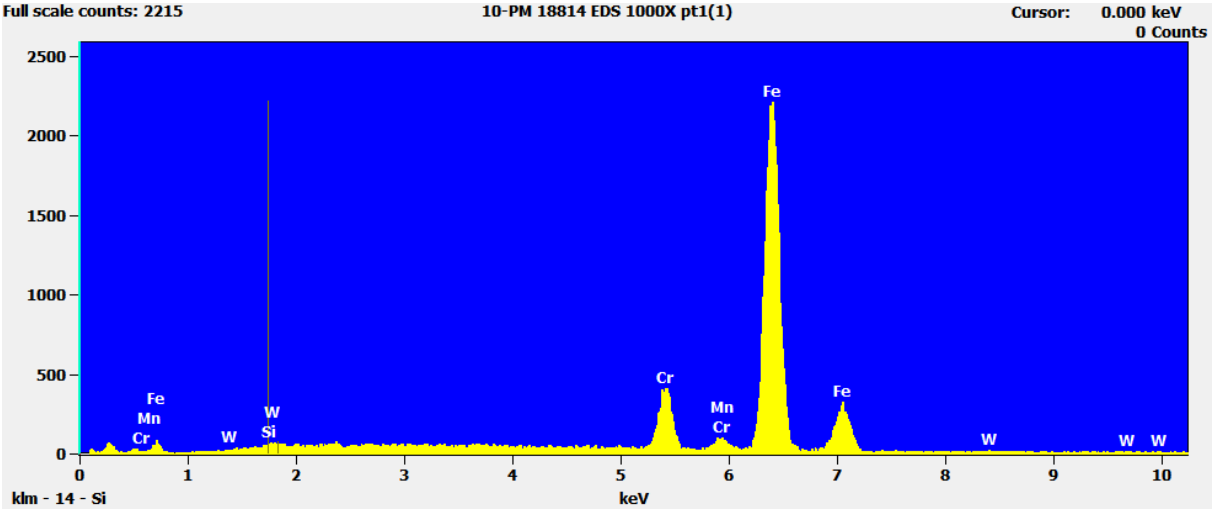

Figure 18: EDS spectrum obtained at specimen #10 surface

Table 5: elements concentration at specimen #10 surface from the EDS analysis.
Filter Fit, Chi² value: 4.254, Correct. Method: Proza (Phi-Rho-Z), Acc.Voltage: 20.0 kV, Take Off Angle: 90.0°.

Element	Weight conc. %	Atomic conc. %
Cr	8.5	9.1
Mn	0.8	0.9
Fe	88.9	89.5
W	1.8	0.5

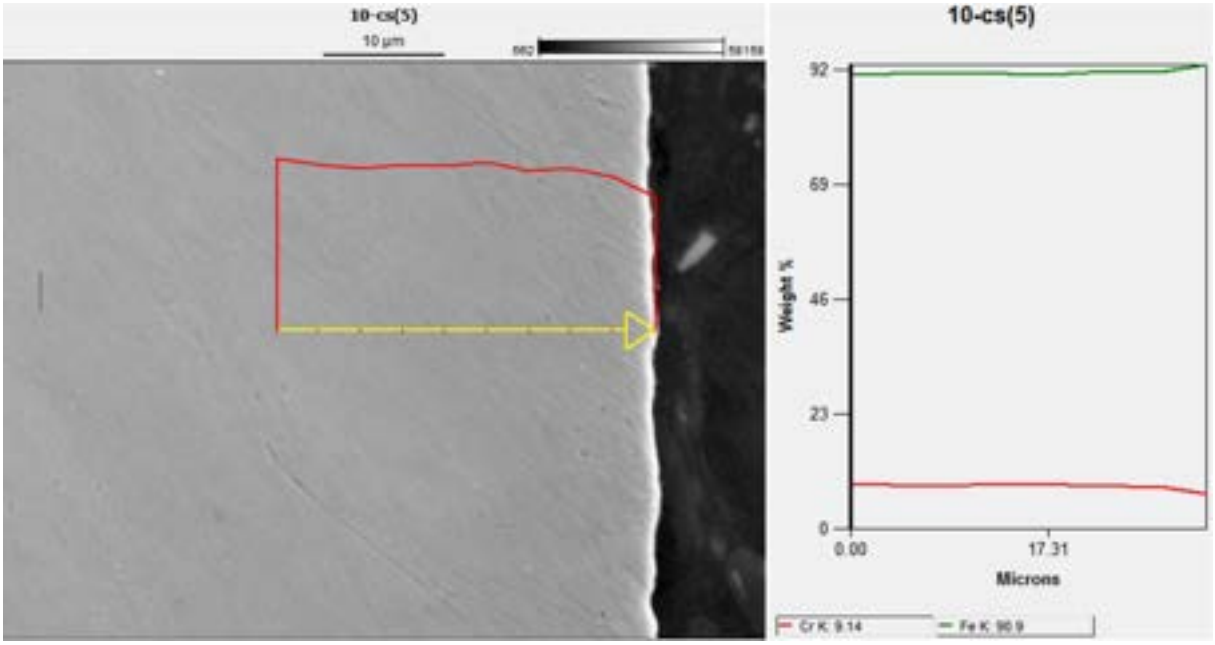

Figure 19: left: SEM image and Cr concentration profile (EDS) of specimen #10 section; right: Cr (red) and Fe (green) concentration profiles along the specimen section.

2.4.5.2 Eurofer 97: specimen #12 (2000 hours)

Figures 20 and 21 show, respectively at magnitude 400 and 2000X, a portion of the external surface of this specimen. Apart from the usual stripes produced during the mechanical manufacturing of the sample, no significant morphological alteration, ascribable to corrosion phenomena, is seen.

Figure 22 depicts instead, at magnitude 2000X, another different region of the external specimen surface. Also in this region, no corrosion item is detected.

By comparing Figures 21 and 22 with the bottom half of Figure 17 (observations made at the same magnitude) it appears anyway a more 'granulose' profile of the specimen #12 surface compared to the fresh one.

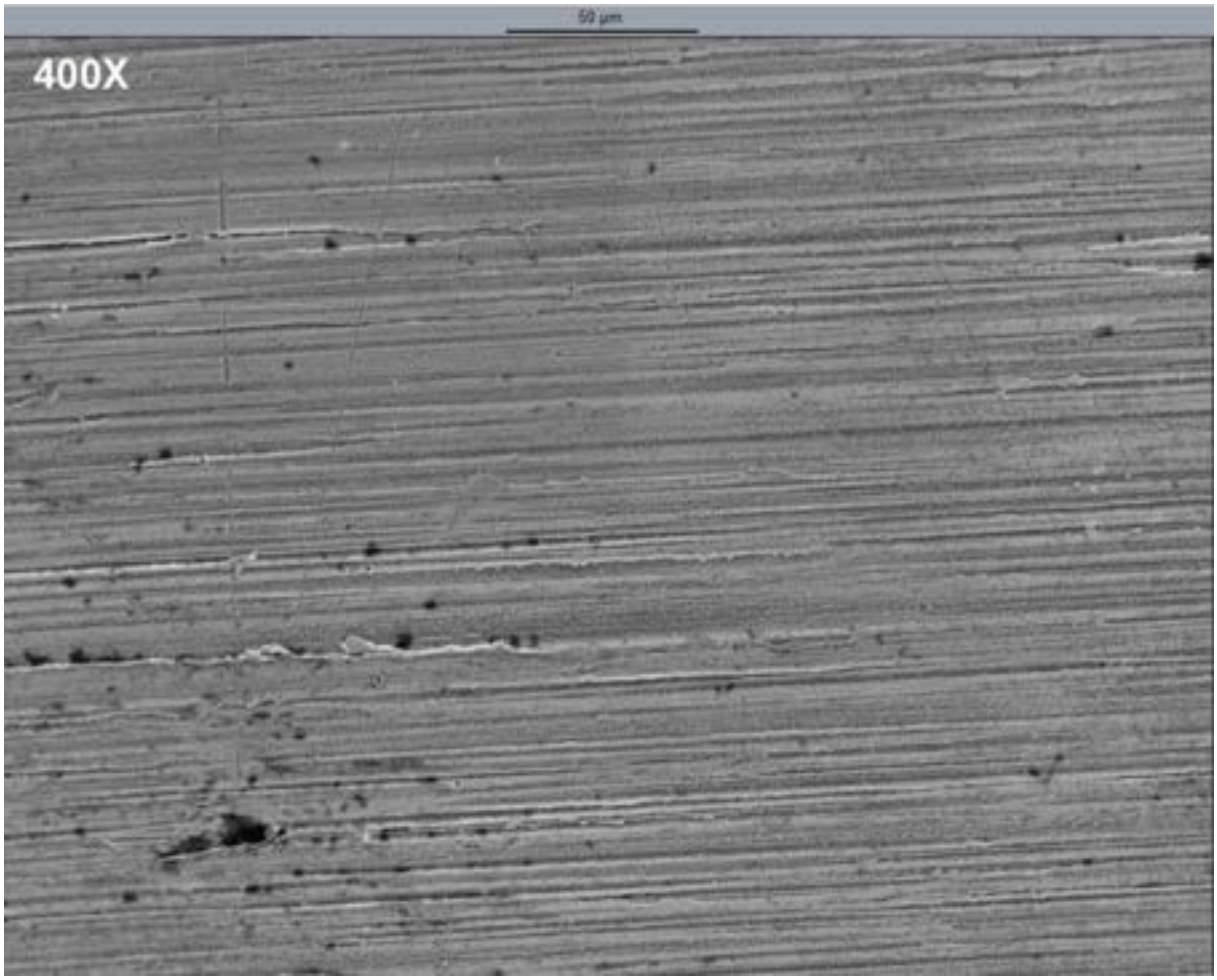

Figure 20: SEM image of specimen #12 surface (secondary electrons) at magnitude 400 X. Scale bar above the image

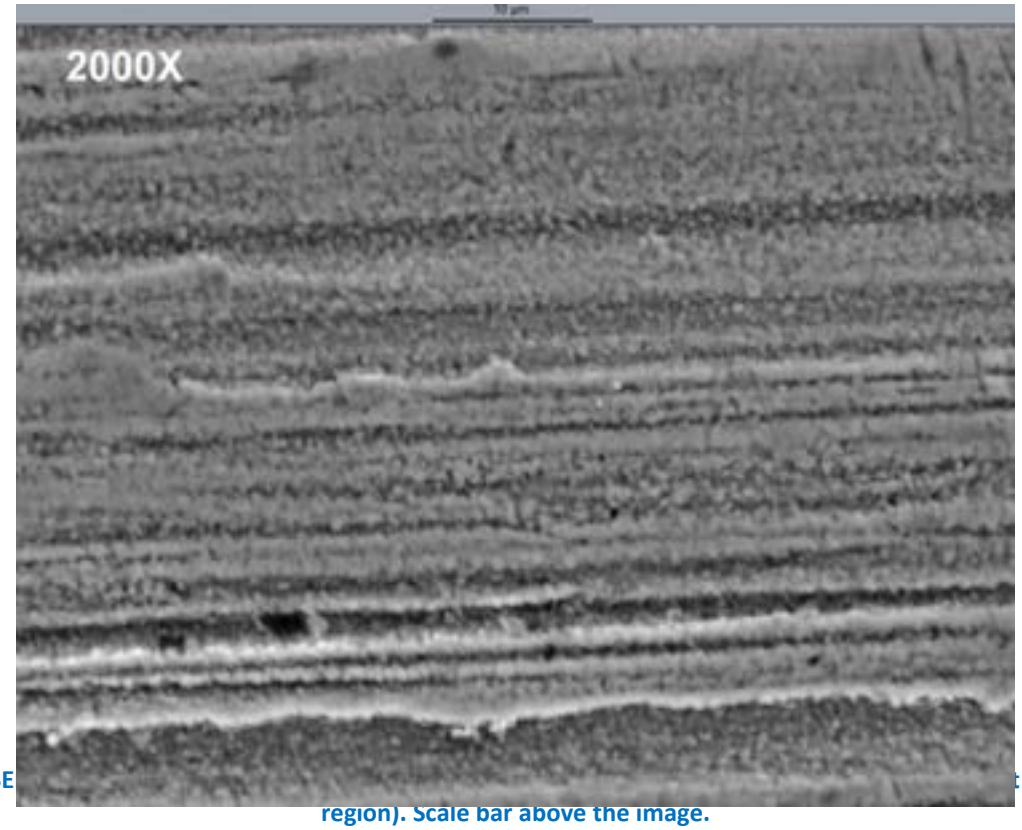

Figure 21: SE[illegible] of Figure 20 region). Scale bar above the image.

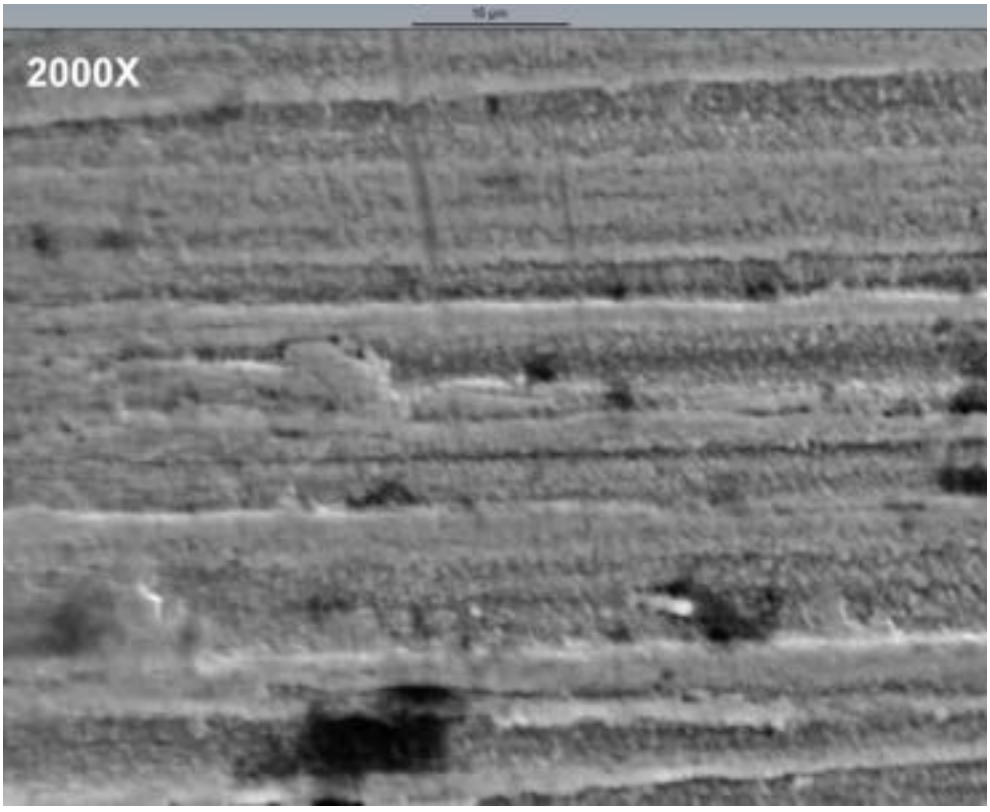

Figure 22: SEM image of another portion of specimen #12 surface (secondary electrons) at magnitude 2000 X. Scale bar above the image.

Figure 23 reports the average EDS spectrum of the external surface region; Table 6 summarizes the values of the related compositional analysis.

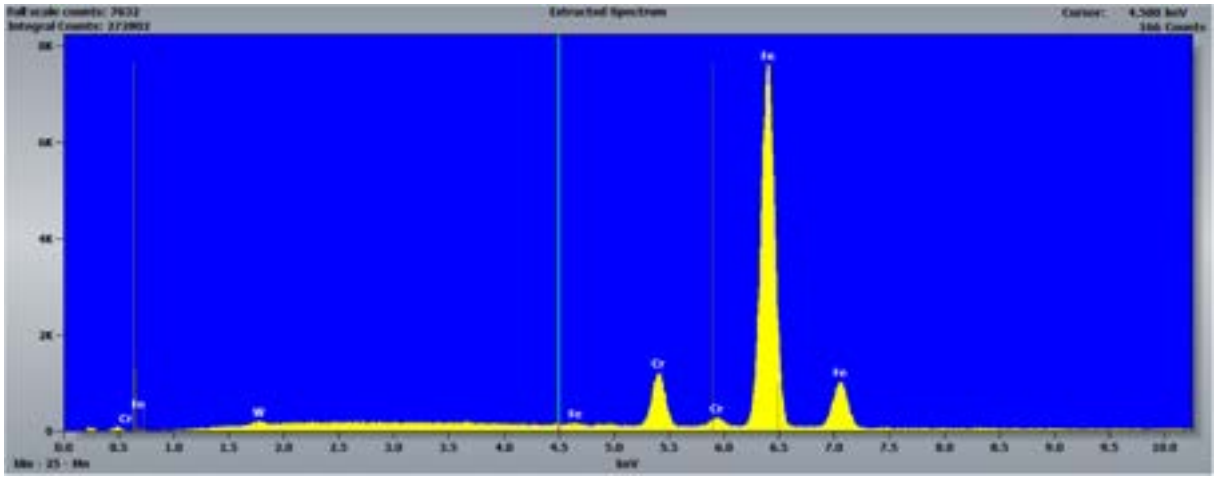

Figure 23: EDS spectrum obtained at specimen #12 surface

Table 6: elements concentration at specimen #12 surface from the EDS analysis.
Filter Fit, Chi² value: 4.254, Correct. Method: Proza (Phi-Rho-Z), Acc.Voltage: 20.0 kV, Take Off Angle: 90.0°.

Element	Weight conc. %	Atomic conc. %
Cr	7.7	8.2
Mn	-	-
Fe	92.3	91.8
W	-	-

From the comparison with Table 5 values, it appears that Mn disappeared at the surface. A W peak is seen in Figure 23 spectrum, but it is very little and under the quantification limit, because almost indistinguishable from the background noise; it was therefore approximated as 0 in the table, indicating again a decrease from the unexposed specimen (#10) value. A depletion is finally measured also in Chromium content (-0.8% by weight). Iron is instead a bit increased, to compensate other elements diminuitions.

Figure 24 (left) shows instead a SEM image at 2000X of a representative cross section of specimen #12, together with the overlapped Chromium concentration vs depth profile, constructed by the EDS analysis of equidistant points (~ 1.5 µm spaced), in the arrow direction. On the right side of Figure 24 is instead reported a graph showing the profiles of both Chromium and Iron elements along the arrow direction, where y-axis is the atomic % concentration, while x-axis indicates the distance from the surface (the surface position is on the left boundary of the graph, in correspondance of x = 0).

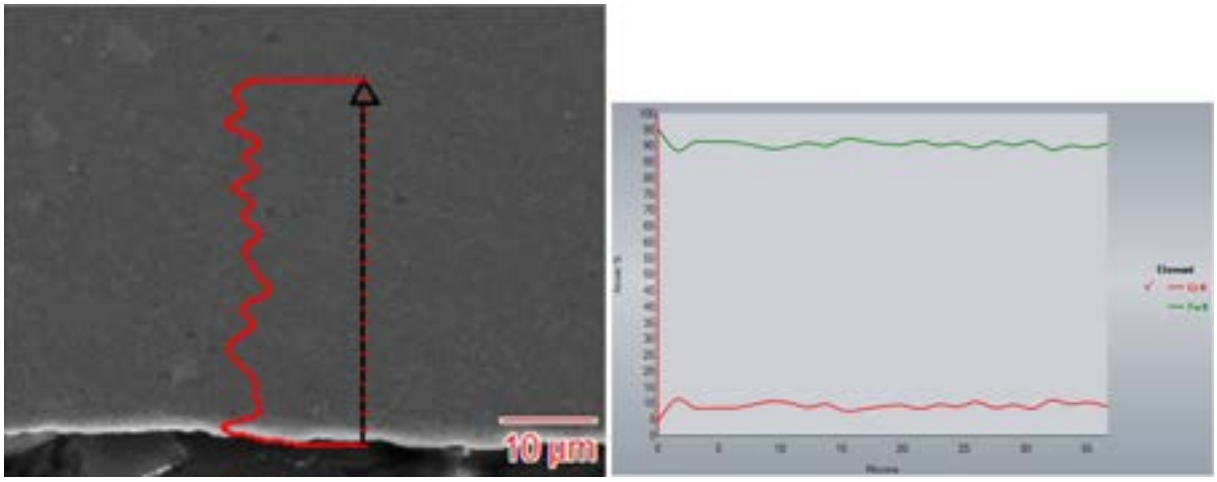

Figure 24: left: SEM image and Cr concentration profile (EDS) of specimen #12 section; right: Cr (red) and Fe (green) concentration profiles along the specimen section.

From the observation of Figure 24 left, it is possible to note that the internal specimen structure is in good condition, with no morphological alteration or grain detachment. The concentration profiles on the right indicate a substantial constancy of values, with only small oscillations due to little random deviations from the theoretical alloy composition and/or to the analysis uncertainty (the starting 'red' value, on the left (Cr), must not be misleading; it is characterized by a value of ~ 5, which is the lowest of all the Cr points, but it is associated to a measurement on the boundary of the sample, so it is not physically meaningful. The first real point is therefore the one of its right, which corresponds to a relative maximum, and from here on Cr concentrations are essentially constant).

2.4.5.3 Eurofer 97: specimen #13 (2000 hours)

Figures 25 and 26 show, at magnitude 400X, 2 different regions of the external surface of this specimen. Region A (Figure 25) is characterized by the absence of degradative phenomena and is exemplifying of the general surface condition; region B (Figure 26) is instead characterized by the presence of some corrosion items (circled in red), which are anyway uncommon on the surface. When enlarging Figure 26 to Figure 27, it is easier to see that these surface anomalies are compatible with a small pitting phenomenon.

In all the shown figures it is possible also to note the presence of remains of organic substances, which originate, as for the other investigated specimens, the black spots in the secondary electrons observations.

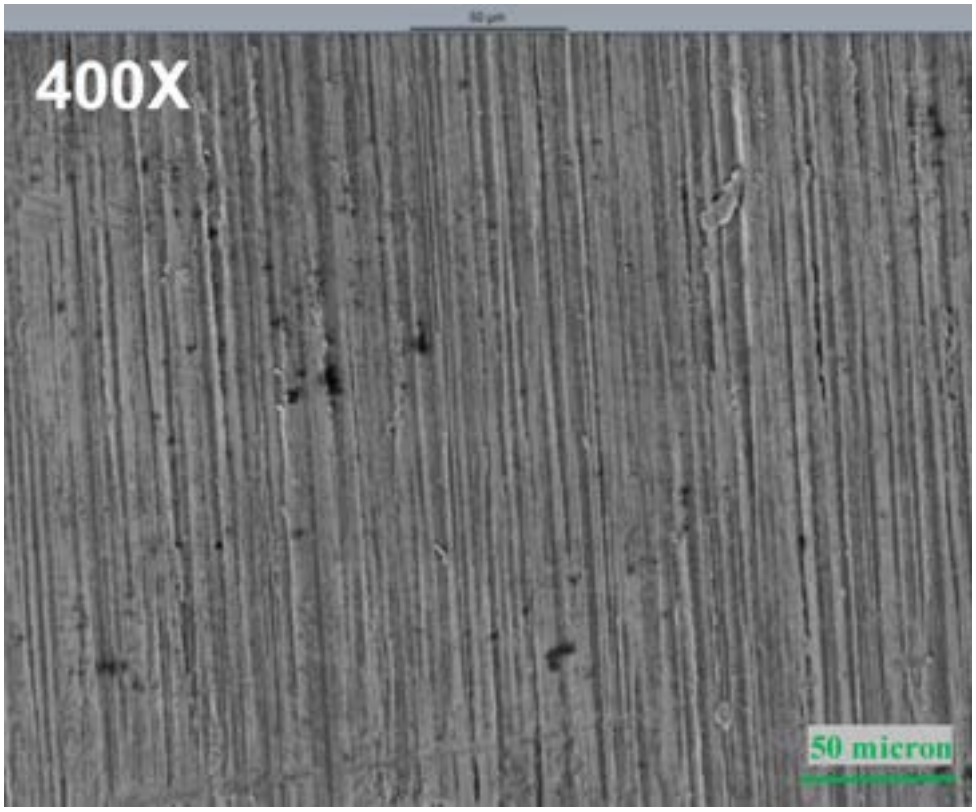

Figure 25: SEM image of region A of specimen #13 surface (secondary electrons) at magnitude 400 X. Scale bar above the image.

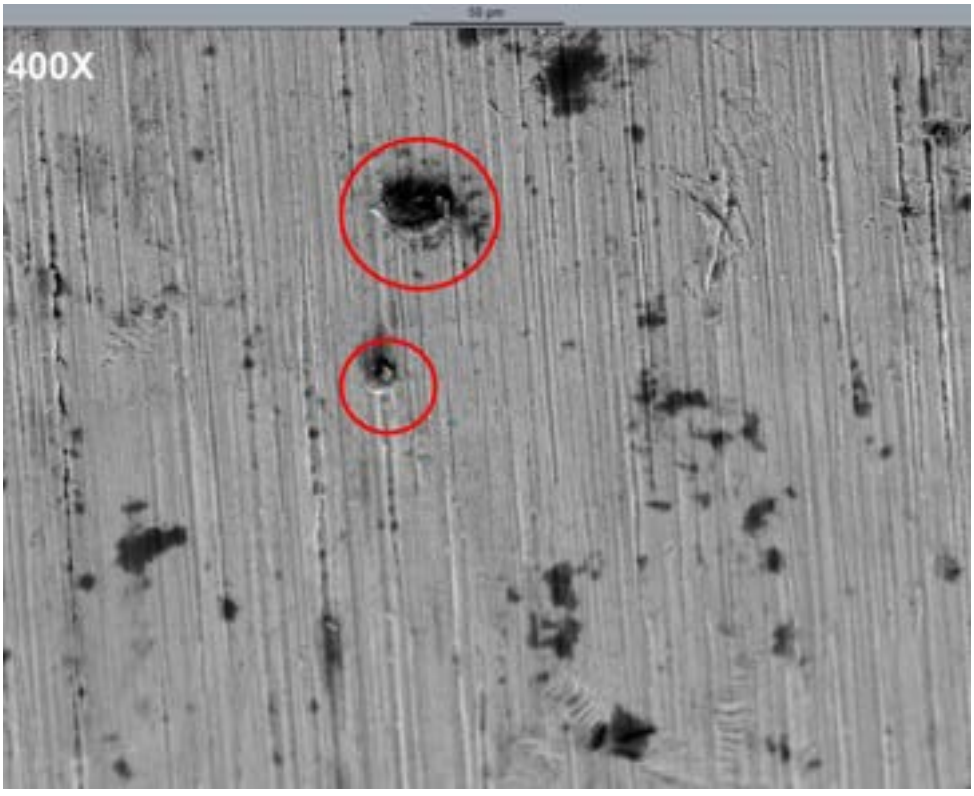

Figure 26: SEM image of region B of specimen #13 surface (secondary electrons) at magnitude 400 X. Scale bar above the image.

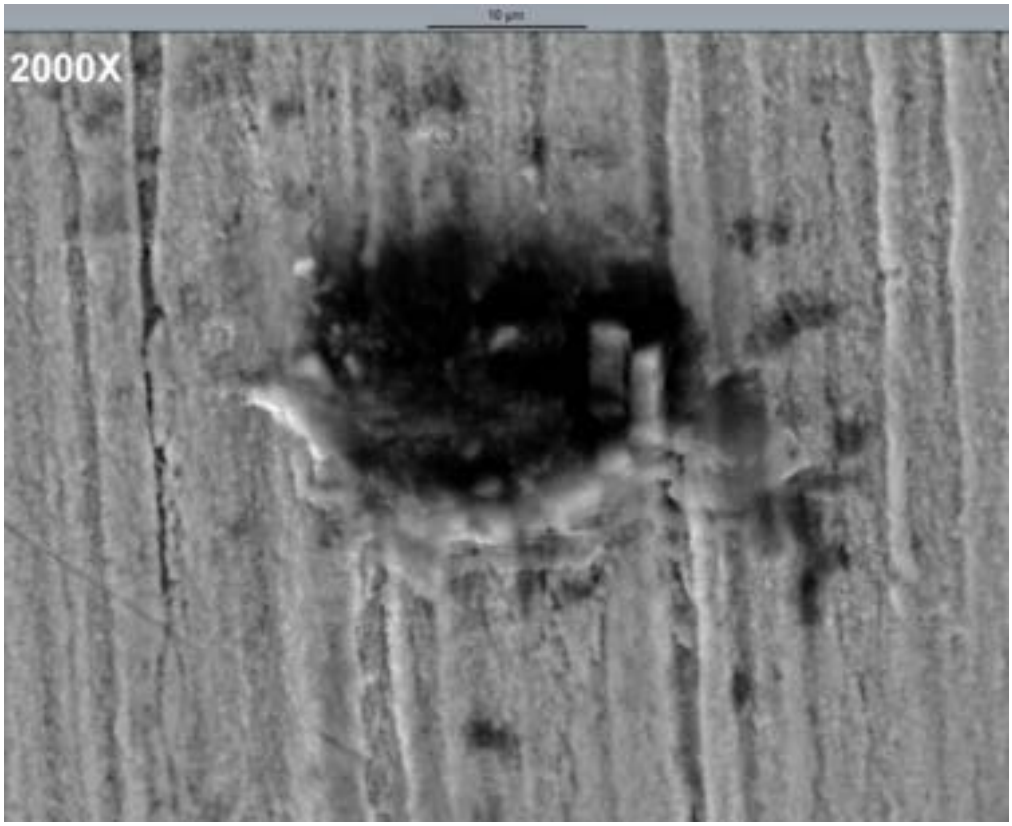

Figure 27: SEM image of region B of specimen #13 surface (secondary electrons) at magnitude 2000 X (enlargement of Figure 26). Scale bar above the image.

Figure 28 reports the average EDS spectrum of an intact portion of a surface region; Table 7 summarizes the values of the related compositional analysis.

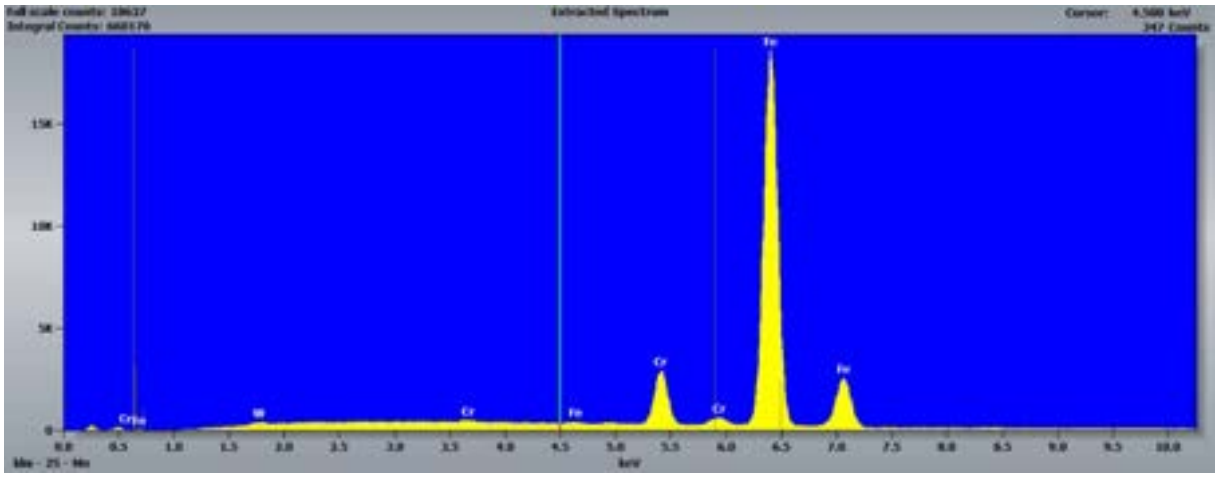

Figure 28: EDS spectrum obtained at specimen #13 surface

Table 7: elements concentration at specimen #13 surface from the EDS analysis.
Filter Fit, Chi² value: 4.254, Correct. Method: Proza (Phi-Rho-Z), Acc.Voltage: 20.0 kV, Take Off Angle: 90.0°.

Element	Weight conc. %	Atomic conc. %
Cr	7.5	8.1
Mn	-	-
Fe	91.3	91.5
W	1.2	0.4

From the comparison with Table 5 values, apart from the Mn disapperance, a depletion of Chromium content at the surface is evident (-1.0% by weight), as already reported for all the other specimens investigated until now.

Figure 29 (left) shows a SEM image at 2000X of a representative cross section of specimen #13, together with the overlapped Chromium concentration vs depth profile, constructed by the EDS analysis of equidistant points (~ 2.2 µm spaced), in the arrow direction. On the right side of Figure 29 is instead reported a graph showing the profiles of both Chromium and Iron elements along the arrow direction, where y-axis is the atomic % concentration, while x-axis indicates the distance from the surface (the surface position is on the left boundary of the graph, in correspondence of x = 0). From the observation of Figure 29 left, it is possible to note that the internal specimen structure is in good condition, with no morphological alteration or grain detachment. The concentration profiles on the right indicate no increasing or decreasing trend of values moving inside the specimen; the starting Cr value, on the left (~ 5), must not be misleading, because it is associated to a measurement on the boundary of the sample, so it is not physically meaningful: the first real point is therefore the one of its right. A part from small values fluctuations, a peak in Cr concentration is seen around 27 µm below the surface. This peak describes a real physical situation, maybe corresponding to a local accumulation of Cr in the form of Carbide; such a kind of compound can be present in the specimen also before the test (in the starting steel composition), therefore it is not indicative of a structure alteration produced by the exposure to flowing Lithium.

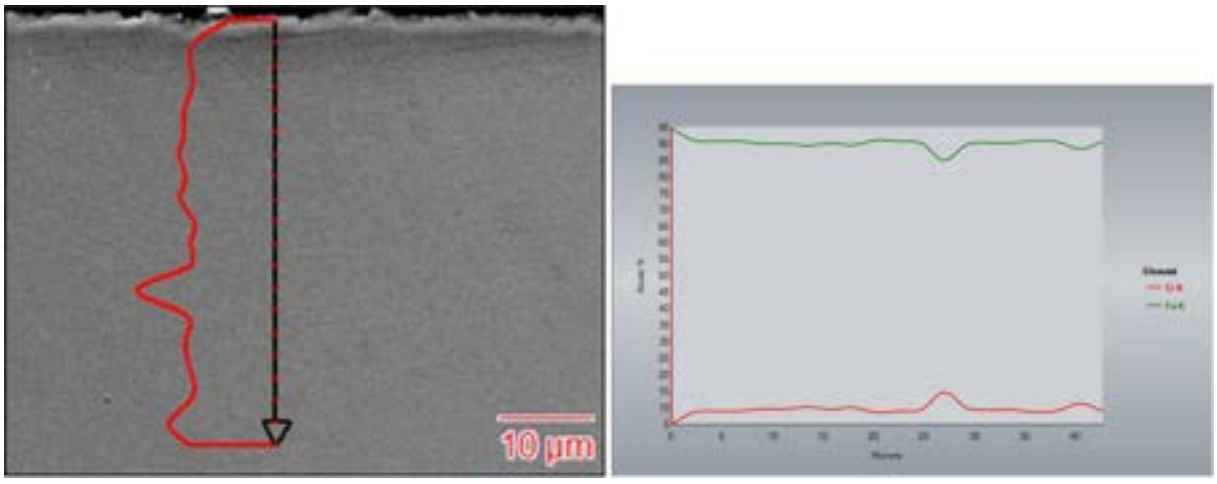

Figure 29: left: SEM image and Cr concentration profile (EDS) of specimen #13 section; right: Cr (red) and Fe (green) concentration profiles along the specimen section.

2.4.5.4 Eurofer 97: specimen #7 (4000 hours)

Figures 30 and 31 show, respectively at magnitude 400 and 2000X, 2 portions of the external surface of this specimen. Apart from the usual stripes produced during the mechanical manufacturing of the sample, no significant morphological alteration, ascribable to corrosion phenomena, is seen. The round black spots, which are seen here as well as in any other investigated specimen, are not due to degradative phenomena of the surface but to external organic substances sticked on the surface. By comparing Figures 31 with the bottom half of Figure 17 (observations made at the same magnitude) it appears anyway a more 'granulose' profile of the specimen #7 surface compared to the fresh one.

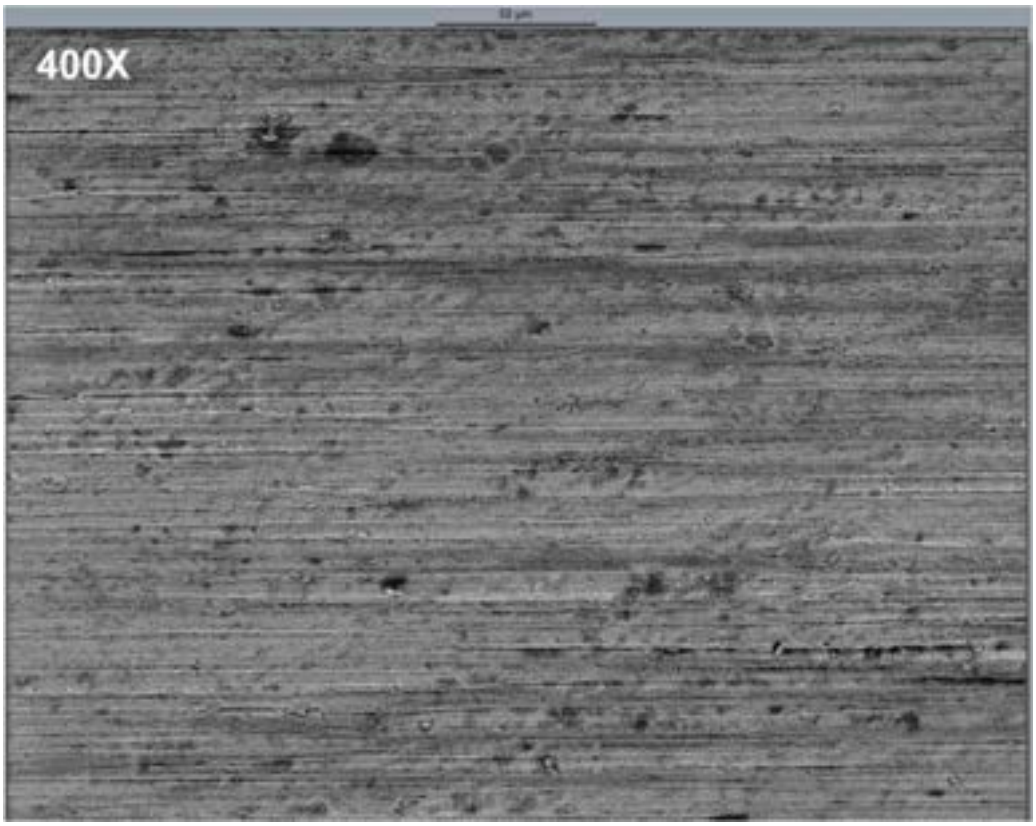

Figure 30: SEM image of specimen #7 surface (secondary electrons) at magnitude 400 X. Scale bar above the image.

Figure 32 reports instead the average EDS spectrum of a large surface region; Table 8 summarizes the values of the related compositional analysis. By looking at Figure 32, the zeroing of Mn and W is evident. Moreover, by comparing Table 8 with Table 5, the Chromium depletion is observed (-1.2% by weigth); Iron content is instead a bit increase, so to compensate for that diminution.

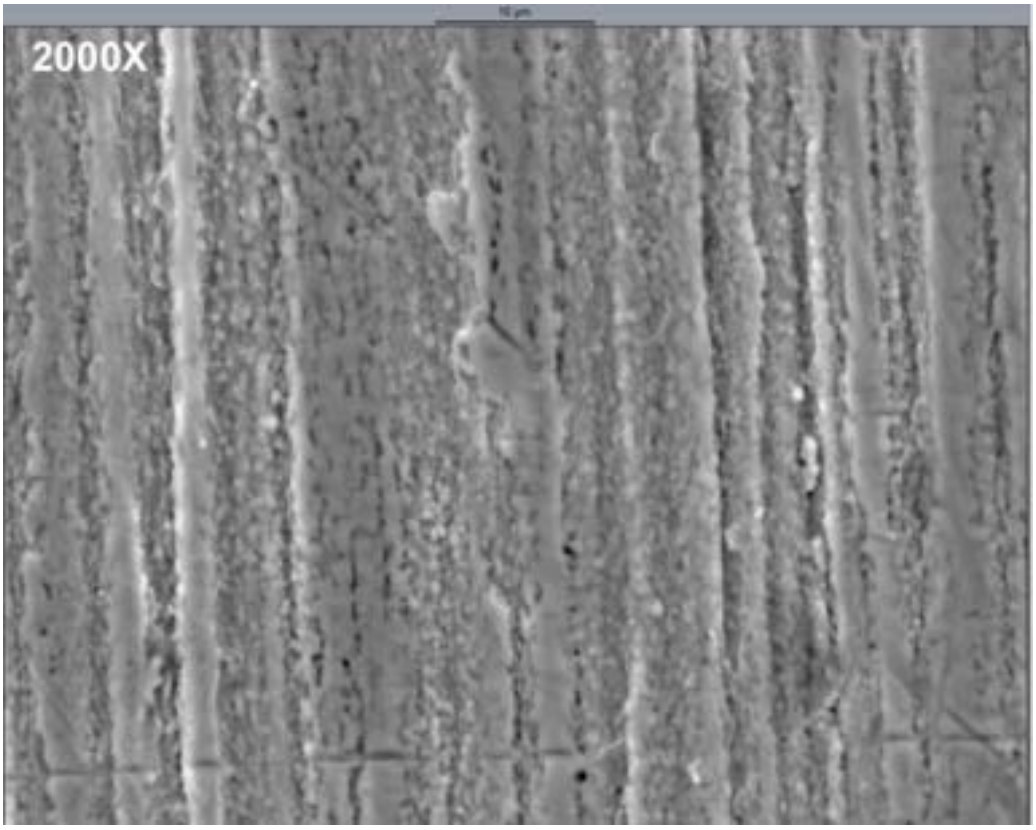

Figure 31: SEM image of specimen #7 surface (secondary electrons) at magnitude 2000 X. Scale bar above the image

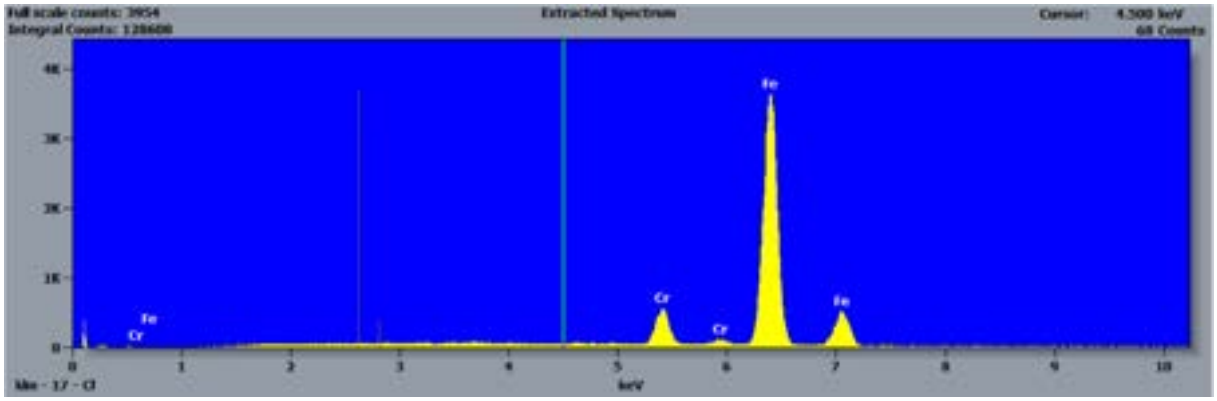

Figure 32: EDS spectrum obtained at specimen #7 surface

Table 8: elements concentration at specimen #7 surface from the EDS analysis.
Filter Fit, Chi² value: 4.254, Correct. Method: Proza (Phi-Rho-Z), Acc.Voltage: 20.0 kV, Take Off Angle: 90.0°.

Element	Weight conc. %	Atomic conc. %
Cr	7.3	7.8
Mn	-	-
Fe	92.7	92.2
W	-	-

Finally, Figure 33 (left) shows a SEM image at 2000X of a representative cross section of specimen #7, together with the overlapped Chromium concentration vs depth profile, constructed by the EDS analysis of equidistant points (~ 2.0 µm spaced), in the arrow direction. On the right side of Figure 33 is instead reported a graph showing the profiles of both Chromium and Iron elements along the arrow direction, where y-axis is the atomic % concentration, while x-axis indicates the distance from the surface (the surface position is on the left boundary of the graph, in correspondence of x = 0). From the observation of Figure 33 left, it is possible to note that the internal specimen structure is in good condition, with no morphological alteration or grain detachment. The concentration profiles on the right indicate no increasing or decreasing trend of values moving inside the specimen; again, the first Cr value, on the left, results smaller than all the other, but only because it is associated to a measurement on the boundary of the sample, which is not physically meaningful. Small oscillations in Cr concentration are due to little local deviations from the theoretical alloy composition and/or to the analysis uncertainty; they are reflected by similar fluctuations of Iron concentrations, since, being other elements absent, Cr+Fe sum always makes 100.

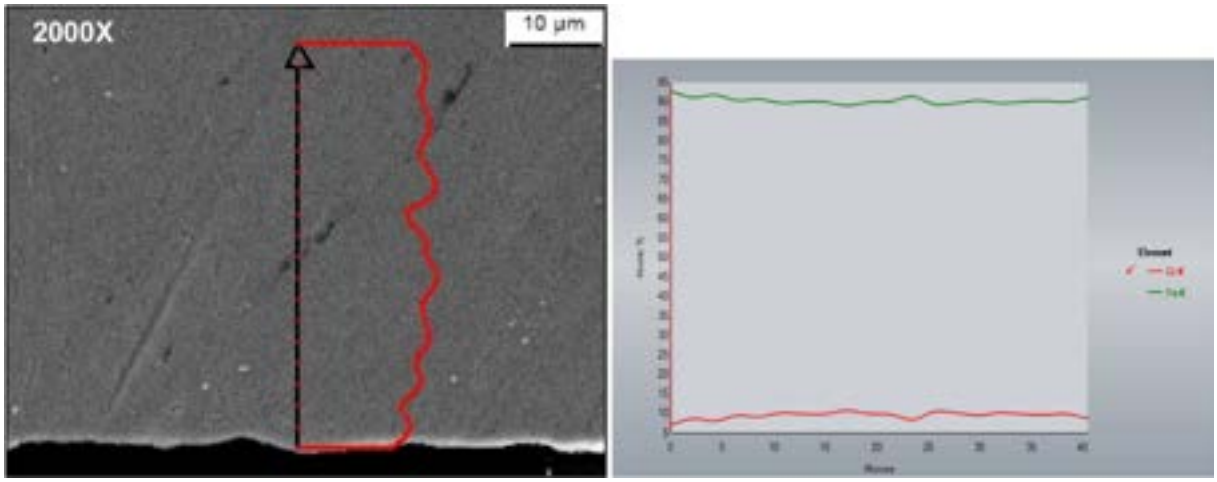

Figure 33: left: SEM image and Cr concentration profile (EDS) of specimen #7 section; right: Cr (red) and Fe (green) concentration profiles along the specimen section.

2.4.5.5 Eurofer 97: specimen #8 (4000 hours)

Figures 34 shows, at magnitude 400X, a portion of the external surface of this specimen. The surface presents the usual features already observed in the other investigated specimens, including also the fresh Eurofer 97 (specimen #10): stripes produced during the manufacturing and black spots due to sticked organic substances. No corrosion item is clearly seen, a part, perhaps, the two small anomalies circled in yellow, which appears as shallow cavities.

Figure 35 is instead a higher magnitude image (2000X) of another surface region. No alteration ascribable to corrosion phenomenon is detected here; it is however possible to note the general aspect of the surface, which results more granulose than before the exposure to the flowing liquid Lithium (by comparing with specimen #10 surface: Figure 17).

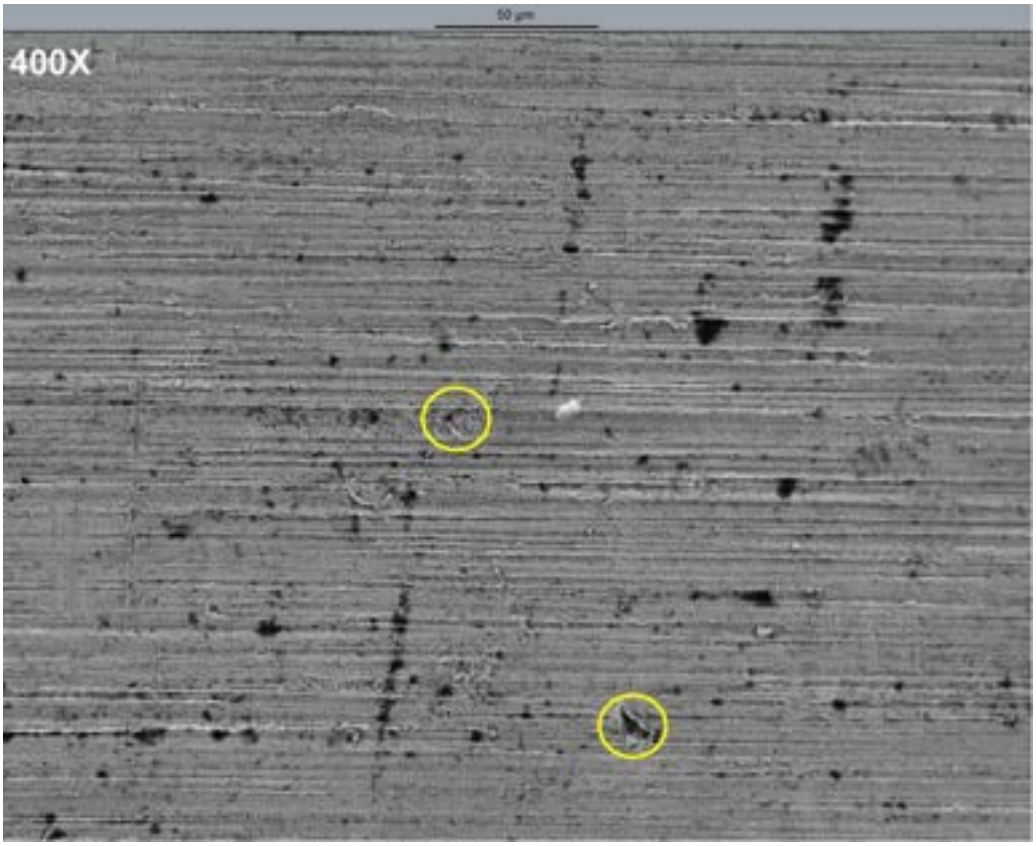

Figure 34: SEM image of specimen #8 surface (secondary electrons) at magnitude 400 X. Scale bar above the image.

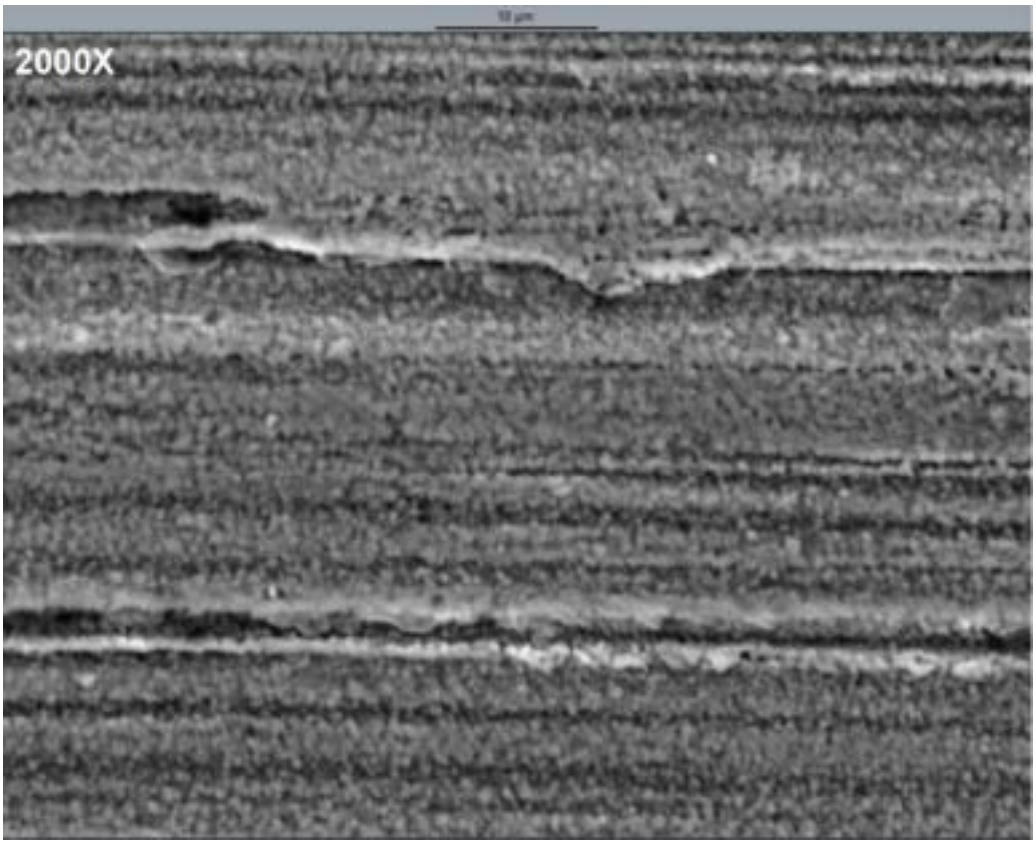

Figure 35: SEM image of specimen #8 surface (secondary electrons) at magnitude 400 X. Scale bar above the image.

Figure 36 reports the average EDS spectrum of a large surface region; Table 9 summarizes the values of the related compositional analysis. The concentration values reported in this table are exactly the same reported in Table 8: same considerations hold.

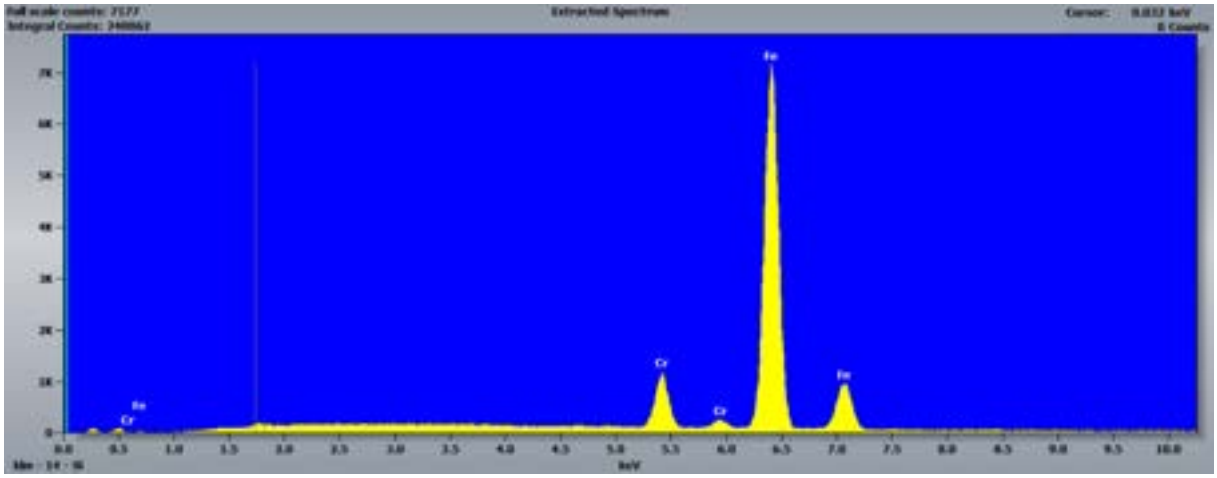

Figure 36: EDS spectrum obtained at specimen #8 surface

Table 9: elements concentration at specimen #8 surface from the EDS analysis.
Filter Fit, Chi² value: 4.254, Correct. Method: Proza (Phi-Rho-Z), Acc.Voltage: 20.0 kV, Take Off Angle: 90.0°.

Element	Weight conc. %	Atomic conc. %
Cr	7.3	7.8
Mn	-	-
Fe	92.7	92.2
W	-	-

Finally, Figure 37 (left) shows a SEM image at 2000X of a representative cross section of specimen #8, together with the overlapped Chromium concentration vs depth profile, constructed by the EDS analysis of equidistant points (~ 2.2 µm spaced), in the arrow direction. On the right side of Figure 37 is instead reported a graph showing the profiles of Chromium, Iron and (this time) also Mn elements along the arrow direction, where y-axis is the atomic % concentration, while x-axis indicates the distance from the surface (the surface position is on the left boundary of the graph, in correspondence of x = 0). From the observation of Figure 37 left, it is possible to note that the internal specimen structure is in good condition, with no morphological alteration or grain detachment. The concentration profiles on the right indicate no increasing or decreasing trend of values moving inside the specimen. Small oscillations in Cr concentration are due to little local deviations from the theoretical alloy composition and/or to the analysis uncertainty; Mn concentration assumes of course very small values, according to the theoretical alloy composition and only in few cases it can be considered different from 0.

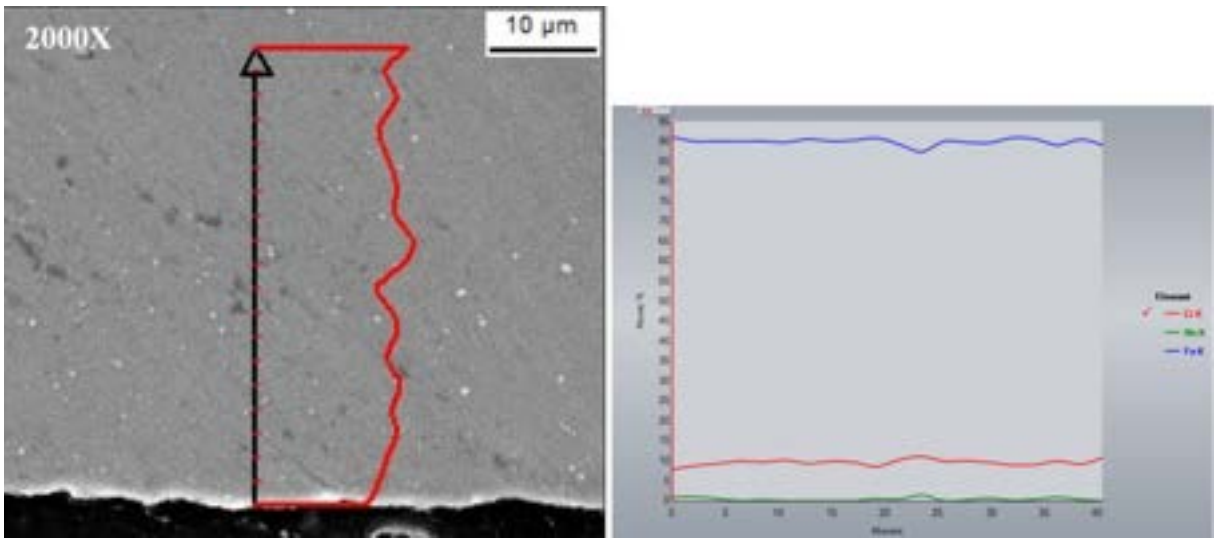

Figure 37: left: SEM image and Cr concentration profile (EDS) of specimen #8 section; right: Cr (red), Fe (blue) and Mn (green) concentration profiles along the specimen section.

2.4.5.6 F82H: specimen #31 (unexposed)

Now, let's look at the F82H specimens, starting with the one not submitted to the erosion-corrosion action by the flowing liquid Lithium (fresh specimen, #31). The related results and observations were already presented in [3] and are here synthetically reminded to allow an easier comparison with the tested specimens.

Figure 38 shows, at different magnitudes, the surface of a representative region of this specimen. As already observed for the Eurofer 97 specimens, also here the sample surface is characterized by the presence of signs due to the mechanical manufacturing, while surface alterations due to erosion-corrosion by Lithium are (of course) absent.

Figure 39 reports the average EDS spectrum of a large area of specimen #31 surface; Table 10 summarizes the values of the related semiquantitive analysis (average composition of the investigated area).

In [3] it was also shown that, differently from the above average composition, white particles like the ones visible in the top part of Figure 38 are characterized by a significant concentration of O, Na and mostly C and Ca (maybe some residue of alkaline carbonate). Since specimen #31 was not exposed to Lithium, surely the presence of the just mentioned elements must be ascribed to the sample handling and its treatment before the execution of the analysis. In any case this conclusion allows to exclude, also for the following, exposed specimens, that similar surface anomalies are somehow consequence of the action exerted by the liquid Lithium.

Finally, Figure 40 shows on the left a SEM representative image of specimen #31 section, with the red Chromium concentration profile overlapped, as determined by the EDS analysis of distinct points (spaced ~ 1.5 µm) in the yellow arrow direction; on the right side is instead reported a graph showing the profiles of both Chromium and Iron weight concentrations. x = 0 in this graph corresponds to the inner position inside the specimen (origin of the arrow).

From the observation of the Figure, it is possible to note that the internal specimen structure is in good condition, with only some sign due to the cut and preparation of the sample, but no erosion-corrosion damage: this is of course what expected, since specimen #31 is an unexposed specimen. The concentration profiles indicate a substantial constancy of values, with minimal fluctuations due to the uncertainty in the EDS analysis result.

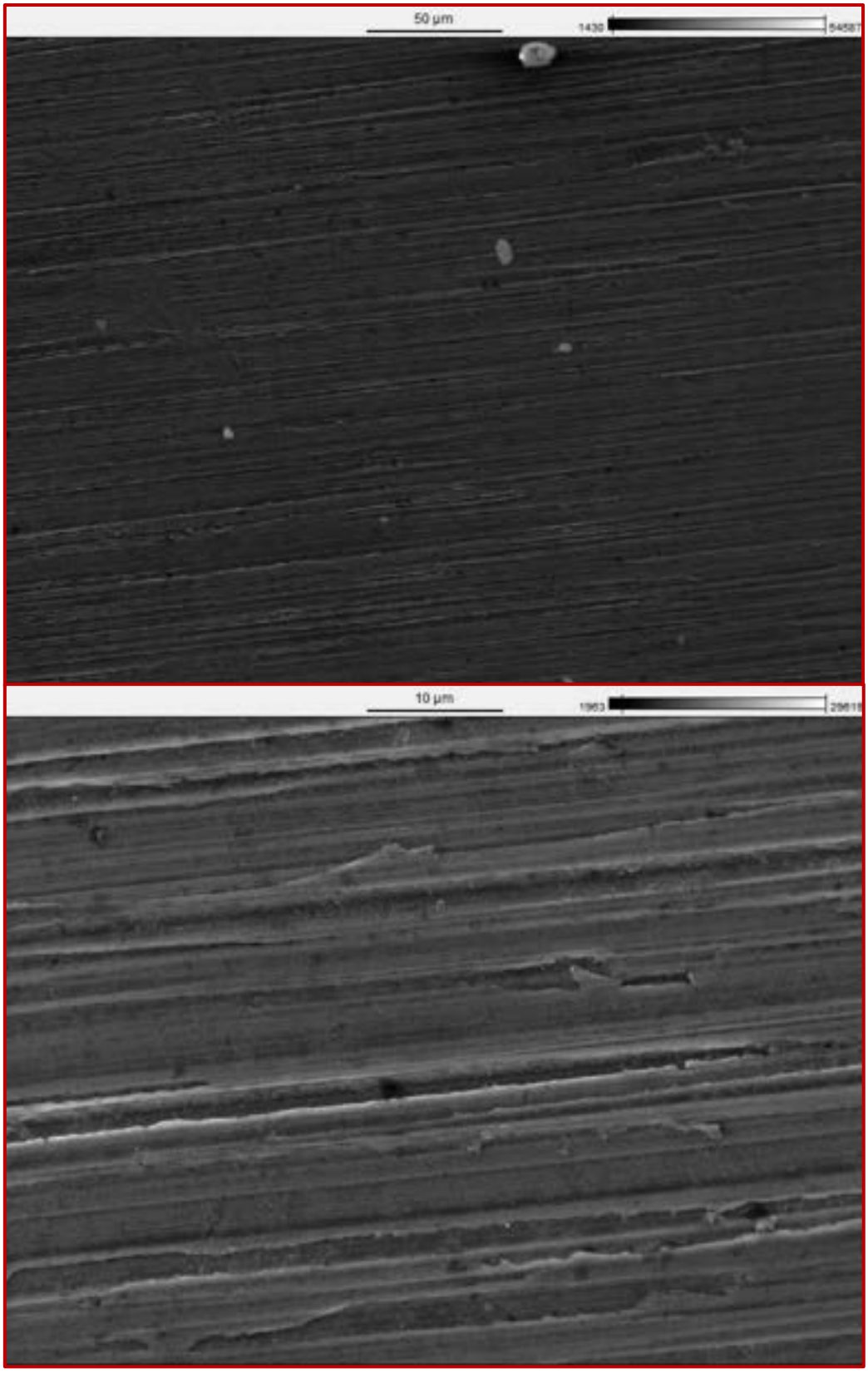

Figure 38: SEM images of specimen #31 surface (secondary electrons) at magnitude 400X (top) and 2000X (bottom). Scale bars above the images.

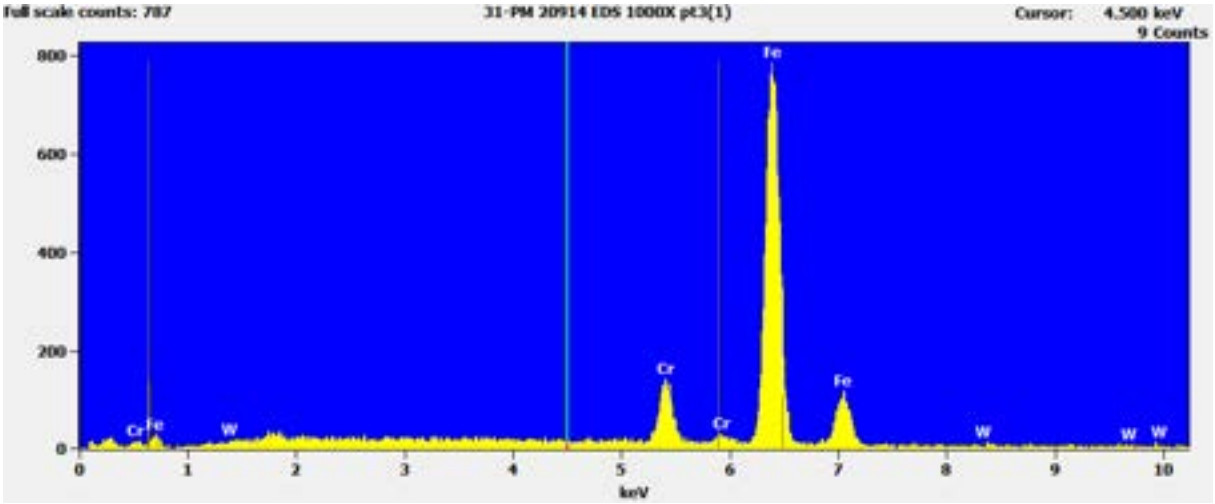

Figure 39: EDS spectrum obtained at specimen #31 surface

Table 10: elements concentration at specimen #31 surface from the EDS analysis.
Filter Fit, Chi² value: 4.254, Correct. Method: Proza (Phi-Rho-Z), Acc.Voltage: 20.0 kV, Take Off Angle: 90.0°.

Element	Weight conc. %	Atomic conc. %
Cr	8.0	8.7
Fe	88.5	90.2
W	3.5	1.1

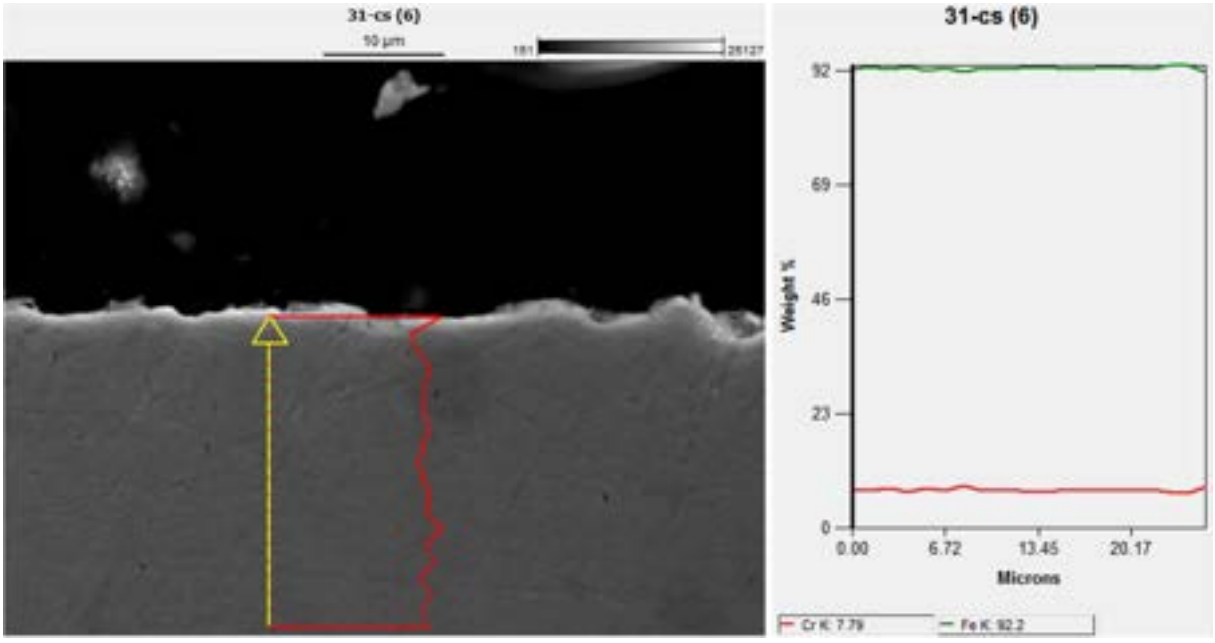

Figure 40: left: SEM image and Cr concentration profile (EDS) of specimen #31 cross section; right: Cr (red) and Fe (green) concentration profiles along the specimen section.

2.4.5.7 F82H: specimen #32 (2000 hours)

Figures 41 and 42 show, respectively at magnitude 400 and 2000X, 2 portions of the external surface of this specimen.

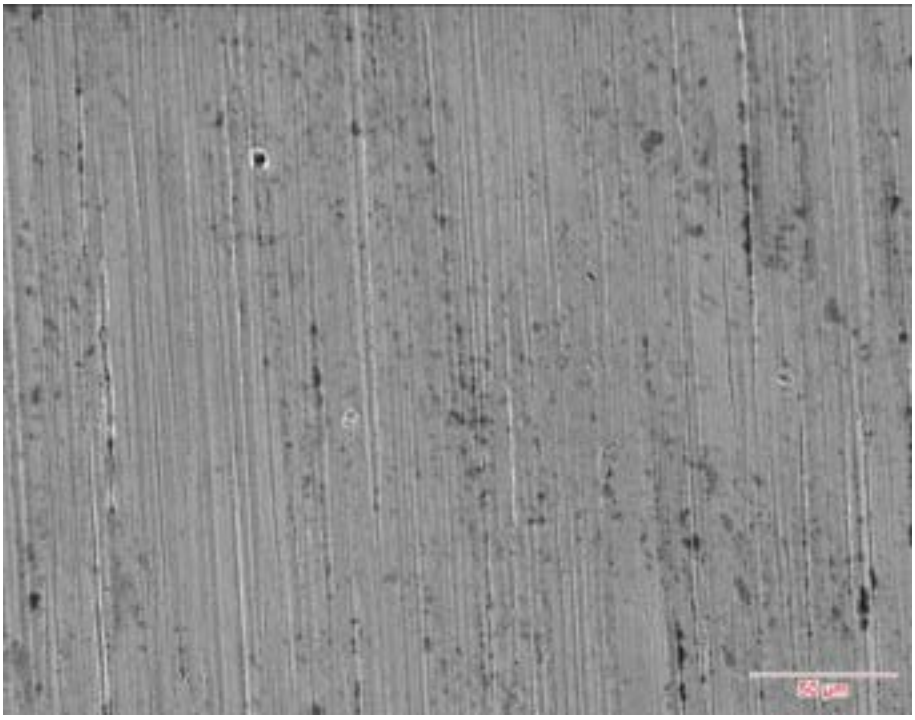

Figure 41: SEM image of specimen #32 surface (secondary electrons) at magnitude 400X. Scale bar above the image.

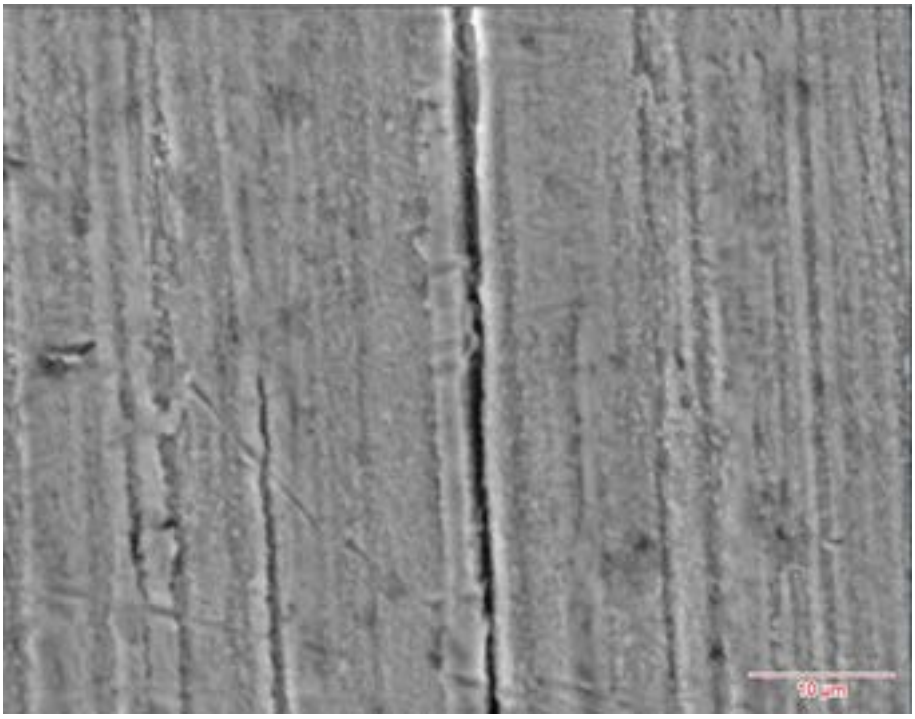

Figure 42: SEM image of spec. #32 surface (secondary electrons) at magnitude 2000X. Scale bar above the image.

Apart from the usual stripes produced during the mechanical manufacturing of the sample, no significant morphological alteration, ascribable to corrosion phenomena, is seen. By comparing Figure 42 with the bottom half of Figure 38 (observations made at the same magnitude) it appears anyway a more 'granulose' profile of the specimen #32 surface compared to the fresh one.

Figure 43 reports the average EDS spectrum of an external surface region; Table 11 summarizes the values of the related compositional analysis. Looking at the Figure, the peak of W is not easily distinguishable from the background noise, therefore this element concentration was not reported in Table 11. By comparing this table values with Table 10 ones, a Chromium depletion at the surface is also noted, corresponding to -1.1% by weight; Iron is instead a bit increased, to compensate other elements diminuitions.

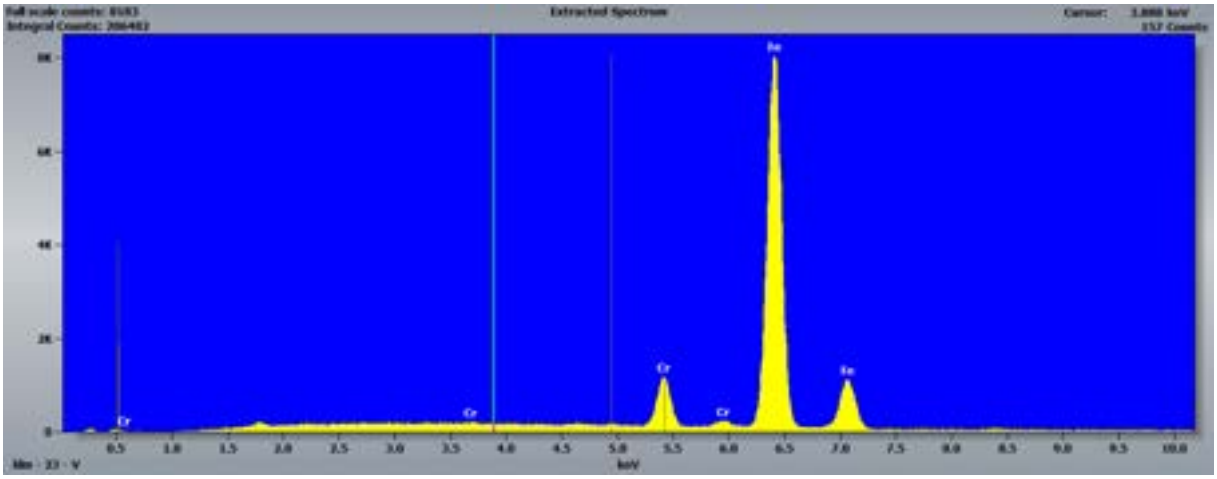

Figure 43: EDS spectrum obtained at specimen #32 surface

Table 11: elements concentration at specimen #32 surface from the EDS analysis.
Filter Fit, Chi² value: 4.254, Correct. Method: Proza (Phi-Rho-Z), Acc.Voltage: 20.0 kV, Take Off Angle: 90.0°.

Element	Weight conc. %	Atomic conc. %
Cr	6.9	7.3
Fe	93.1	92.7
W	-	-

Finally, Figure 44 (left) shows a SEM image at 2000X of a representative cross section of specimen #32, together with the overlapped Chromium concentration vs depth profile, constructed by the EDS analysis of equidistant points (~ 2.2 µm spaced), in the arrow direction. On the right side of Figure 44 is instead reported a graph showing the profiles of Chromium and Iron elements along the arrow direction, where y-axis is the atomic % concentration, while x-axis indicates the distance from the surface (the surface position is on the left boundary of the graph, in correspondence of x = 0). From the observation of Figure 44 left, it is possible to note that the internal specimen structure is in good condition, with no morphological alteration or grain detachment. The concentration profiles on the right indicate no increasing or decreasing trend of values moving inside the specimen. Small oscillations in Cr concentration are due to little local deviations from the theoretical alloy composition and/or to the analysis uncertainty; specular fluctuations are seen in Fe concentration values, since the sum of Cr and Fe makes always 100.

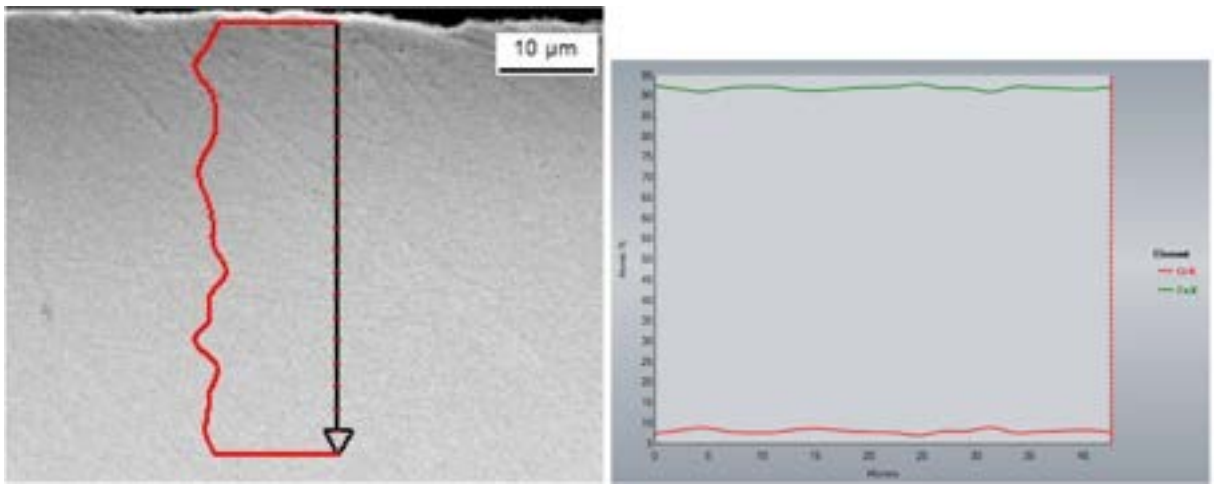

Figure 44: left: SEM image and Cr concentration profile (EDS) of specimen #32 section; right: Cr (red) and Fe (green) concentration profiles along the specimen section.

2.4.5.8 F82H: specimen #34 (2000 hours)

Figures 45 and 46 show, respectively at magnitude 400 and 2000X, 2 portions of the external surface of this specimen. In both these figures are visible the usual signs produced by mechanical manufacturing of the specimens, in the form of vertical stripes, which, at large magnifications, appear as narrow and shallow channels, as well as the black spots associated to sticked organic substances. By comparing Figure 46 with the bottom half of Figure 38 (observations made at the same magnitude), a more 'granulose' profile of the specimen #34 surface compared to the fresh one also appears.

Figure 47 is instead a SEM image (at 800X) of a different region of specimen #34 surface. In this figure a corrosion item, circled in blue, has been decteted; its dimensions are however limited, of the order of 10 µm. The other object, circled in purple, is characterized by larger dimensions and by clear parts, which seem to come off the surface, as well as cavities in correspondance of the darker parts. It could correspond to a kind of precipitate, maybe a metallic carbide already present in the original alloy, which contains metals nobler than Fe and Cr and could have withdraw electrons from them, in presence of a good conductor like liquid Lithium (galvanic corrosion).

Similarly, Figure 48 shows a different surface region (at 4000X), highlighting another alteration of the surface, in the form of small holes produced by corrosion phenomena; its dimensions are again around 10 µm.

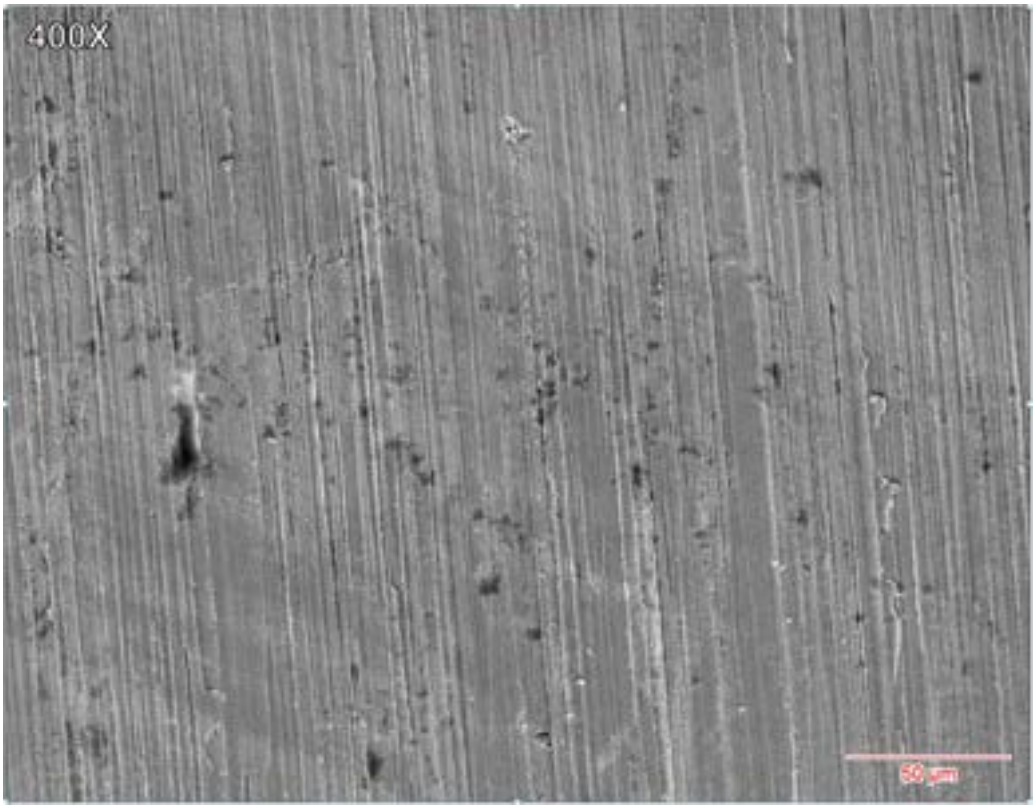

Figure 45: SEM image of specimen #34 surface (secondary electrons) at magnitude 400X. Scale bar above the image.

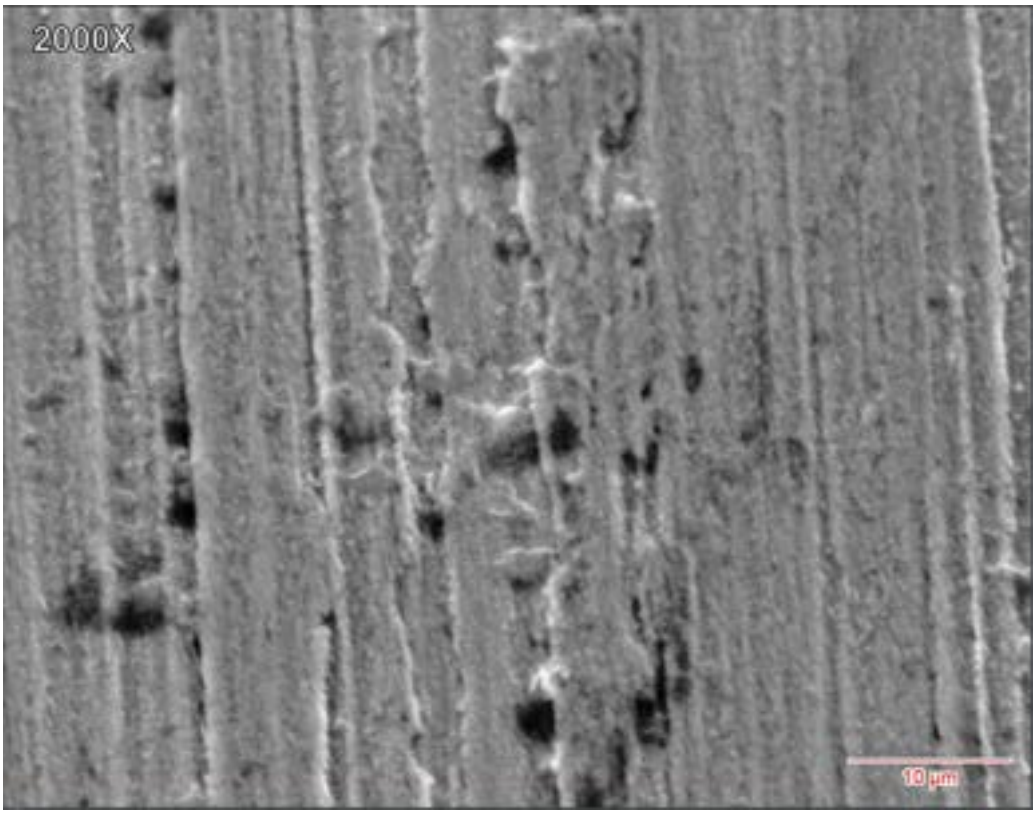

Figure 46: SEM image of spec. #34 surface (secondary electrons) at magnitude 2000X. Scale bar above the image.

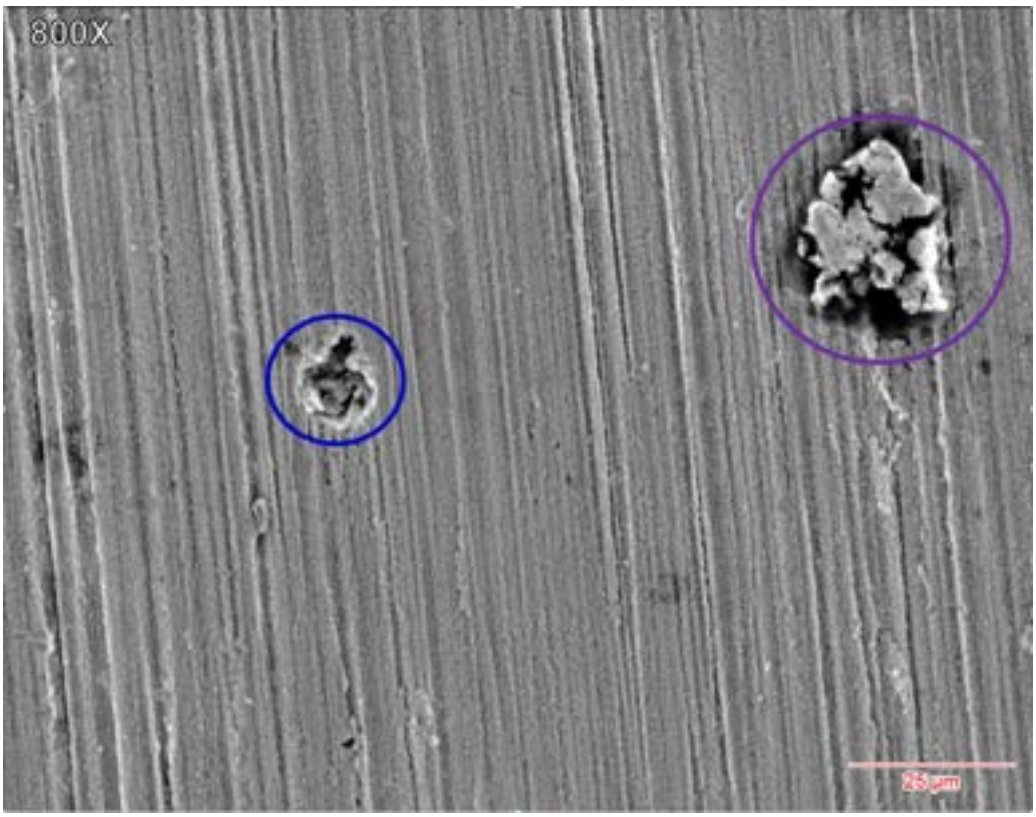

Figure 47: SEM image of specimen #34 surface (secondary electrons) at magnitude 800X, highlighting two surface anomalies. Scale bar above the image.

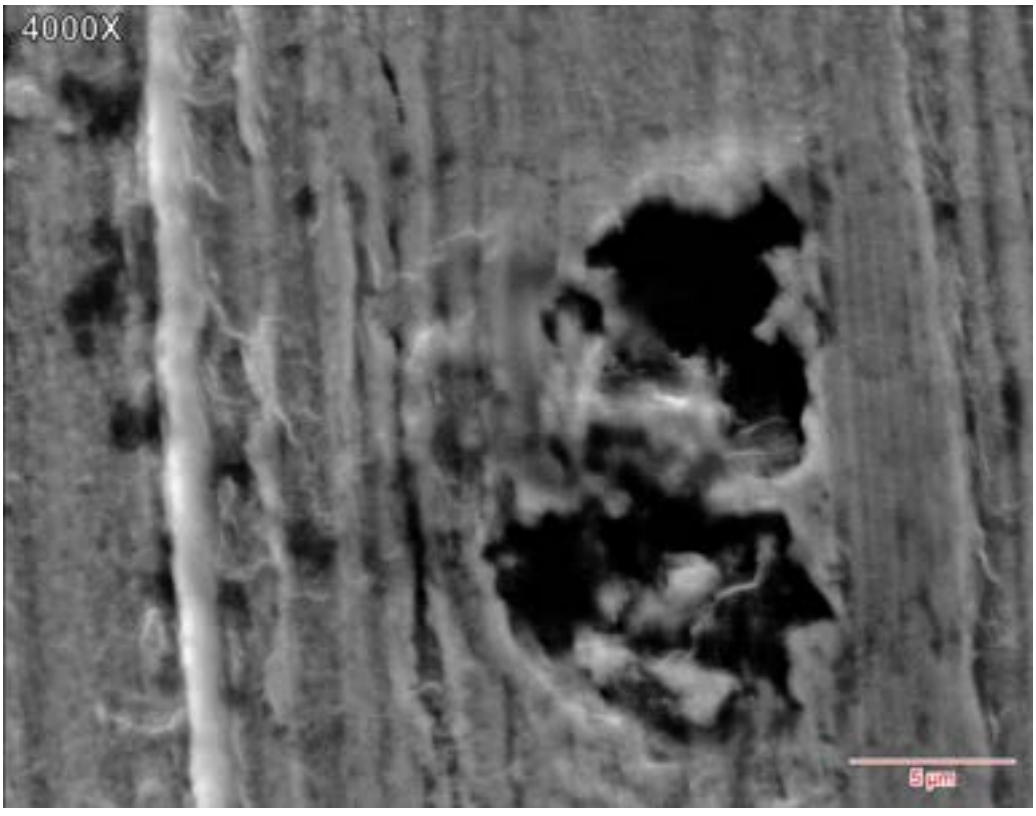

Figure 48: high magnitude (4000X) SEM image of specimen #34 surface (secondary electrons), focused on a riddled surface region. Scale bar above the image.

Figure 49 reports the average EDS spectrum of the whole region; Table 12 summarizes the values of the related compositional analysis. By comparing this table values with Table 10 ones, a Chromium depletion at the surface is also noted, corresponding to -1.5% by weight; Tungsten is below the quantification limit; Iron is instead a bit increased, to compensate other elements diminuitions.

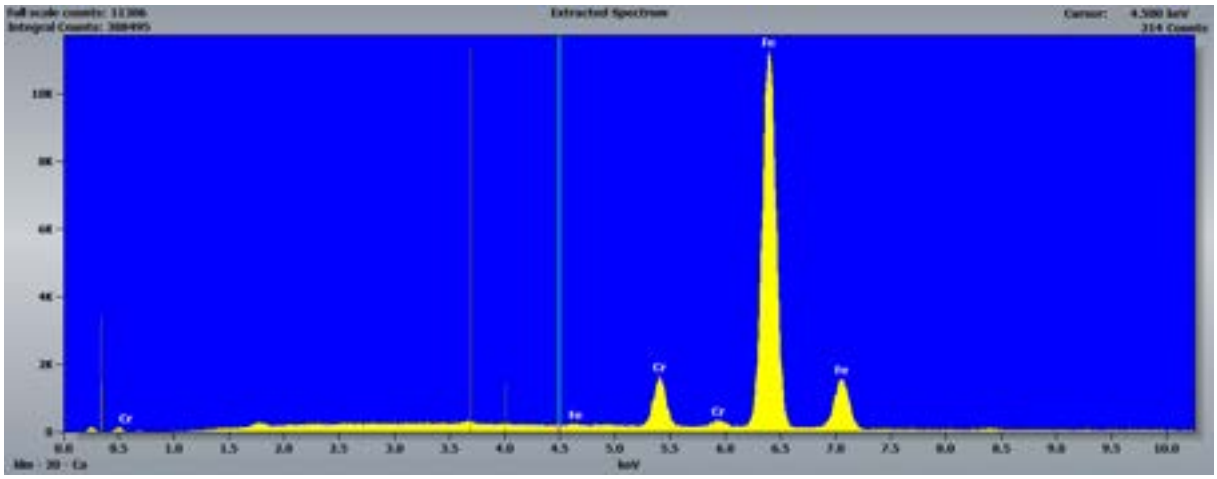

Figure 49: EDS spectrum obtained at specimen #34 surface

Table 12: elements concentration at specimen #34 surface from the EDS analysis.
Filter Fit, Chi² value: 4.254, Correct. Method: Proza (Phi-Rho-Z), Acc.Voltage: 20.0 kV, Take Off Angle: 90.0°.

Element	Weight conc. %	Atomic conc. %
Cr	6.5	7.0
Fe	93.5	93.0
W	-	-

Finally, Figure 50 (left) shows a SEM image at 2000X of a representative cross section of specimen #34, together with the overlapped Chromium concentration vs depth profile, constructed by the EDS analysis of equidistant points (~ 2.2 µm spaced), in the arrow direction. On the right side of Figure 50 is instead reported a graph showing the profiles of Chromium and Iron elements along the arrow direction, where y-axis is the atomic % concentration, while x-axis indicates the distance from the surface (the surface position is on the left boundary of the graph, in correspondence of x = 0). From the observation of Figure 50 left, it is possible to note that the internal specimen structure is in good condition, with no morphological alteration or grain detachment. The concentration profiles on the right indicate no increasing or decreasing trend of values moving inside the specimen. Small oscillations in Cr concentration are due to little random deviations from the theoretical alloy composition and/or to the analysis uncertainty; specular fluctuations are seen in Fe concentration values, since the sum of Cr and Fe makes always 100.

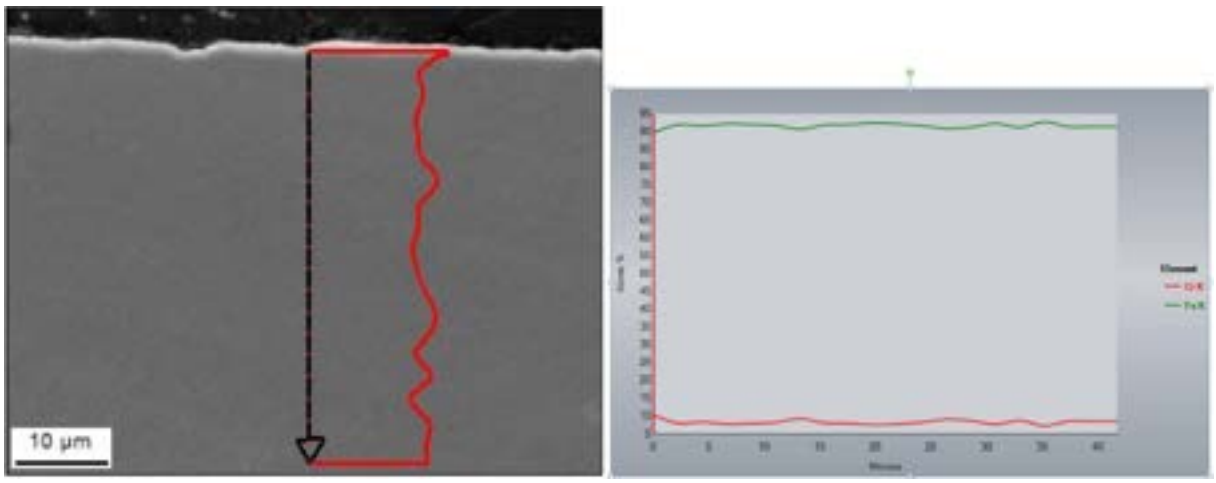

Figure 50: left: SEM image and Cr concentration profile (EDS) of specimen #34 section; right: Cr (red) and Fe (green) concentration profiles along the specimen section.

2.4.5.9 F82H: specimen #28 (4000 hours)

Now let's look at the F82H specimens exposed to flowing Lithium for a total time of 4000 hours, starting with specimen #28. Figures 51 shows, at magnitude 400X, a region of the external surface of this specimen. Apart from the usual vertical stripes produced during the manifacturing of the sample, additional mechanical alterations like scratches and abrasions are visible, which are not indicative however of a corrosion action exerted by Lithium. In the centre of Figure 51 is instead detected a roundish dark object (circled in green), which, especially when observed at higher magnification (Figure 52, 2000X), reveals its nature of cavity originated in response to a corrosion phenomenon.

The average EDS spectrum of a large surface region (~ 160x130 μm^2) around the discussed cavity is shown in Figure 53; Table 13 reports the concentration values calculated from those peaks. Again, as for the previously discussed specimens, the Tungsten surface concentration decreased below the quantification limit, a Chromium depletion was observed (-1.6% by weight) and Iron increased a bit, to compensate other elements diminuitions.

Finally, Figure 54 (left) shows a SEM image at 2000X of a representative cross section of specimen #28, together with the overlapped Chromium concentration vs depth profile, constructed by the EDS analysis of equidistant points (~ 2 µm spaced), in the arrow direction. On the right side of Figure 54 is instead reported a graph showing the profiles of Chromium and Iron elements along the arrow direction, where y-axis is the atomic % concentration, while x-axis indicates the distance from the surface (the surface position is on the left boundary of the graph, in correspondence of x = 0). From the observation of Figure 54 left, it is possible to note that the internal specimen structure is in good condition, with no morphological alteration or grain detachment. The concentration profiles on the right indicate no increasing or decreasing trend of values moving inside the specimen (the first Cr point, on the left extremity, corresponds the smallest concentration value, but it is not physically sure, since measured too close to the border of the specimen). Small oscillations in Cr concentration are due to little local deviations from the theoretical alloy composition and/or to the analysis uncertainty; specular fluctuations are seen in Fe concentration values, since the sum of Cr and Fe makes always 100.

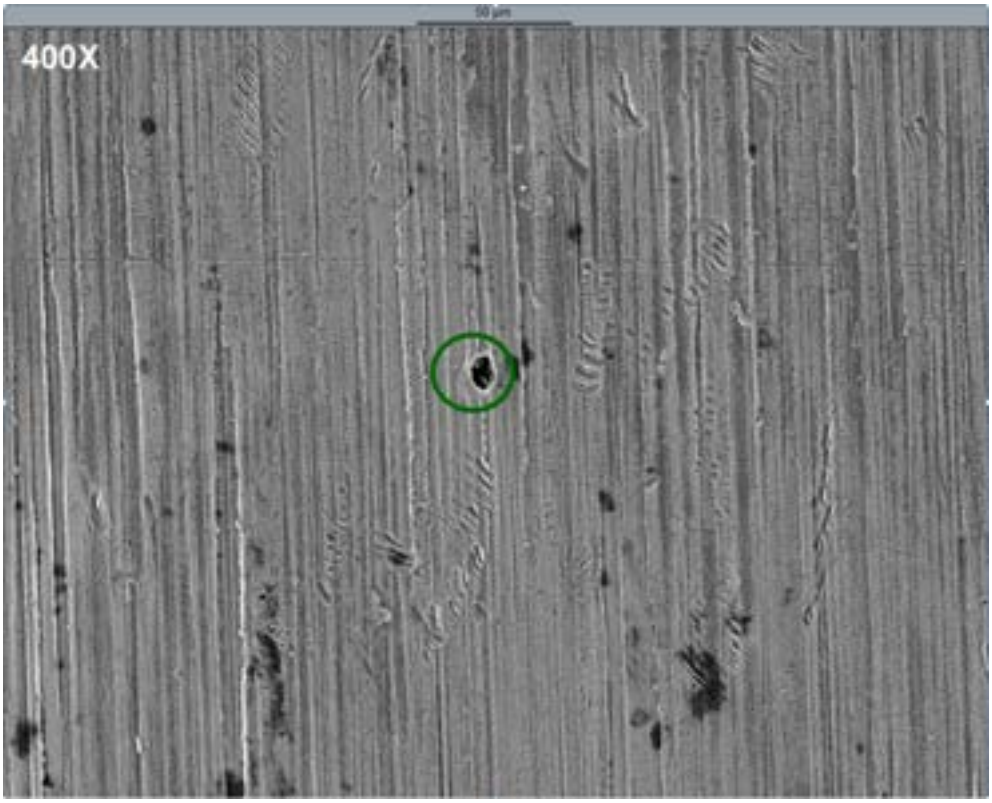

Figure 51: SEM image of specimen #28 surface (secondary electrons) at magnitude 400X. Scale bar above the image

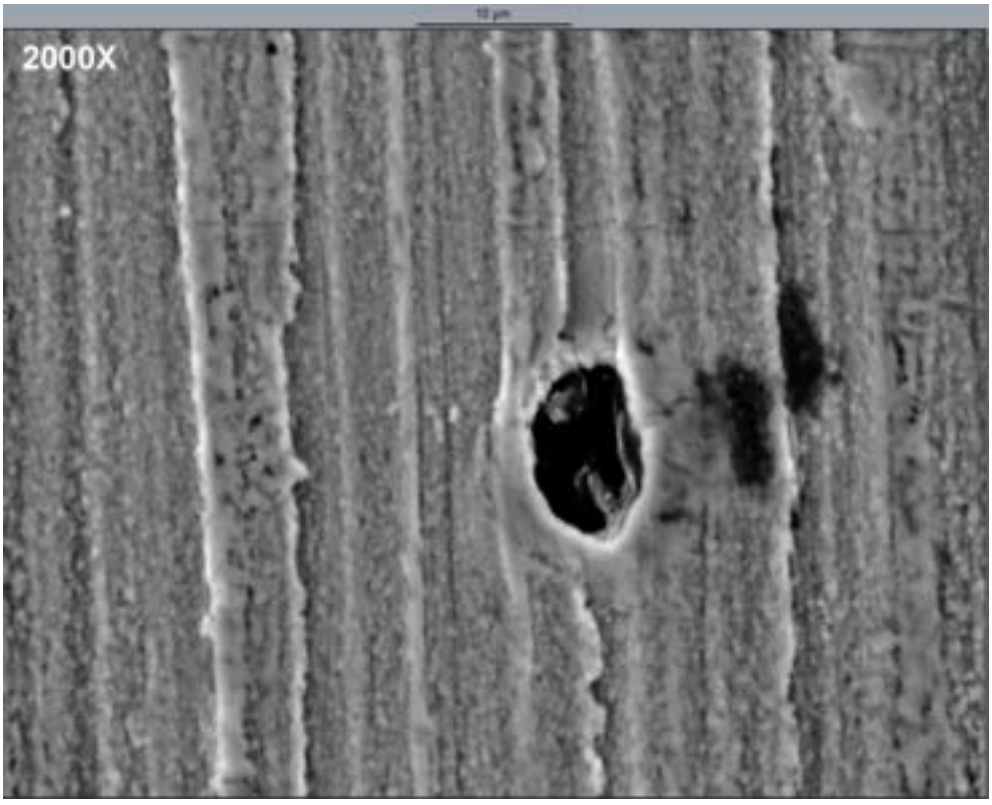

Figure 52: SEM image of specimen #28 surface (secondary electrons) at magnitude 2000X (enlargement of Figure 51 centered on the corrosion item). Scale bar above the image.

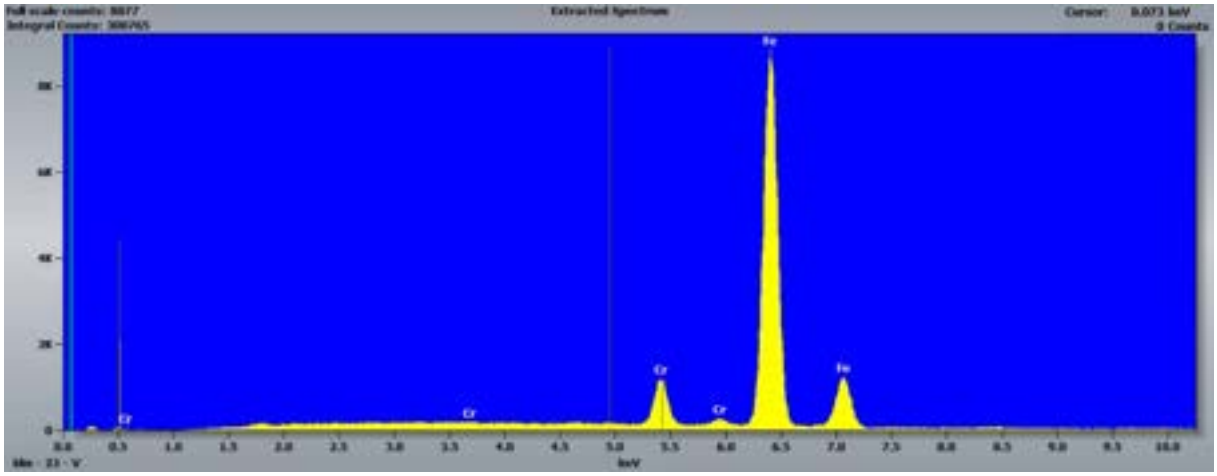

Figure 53: EDS spectrum obtained at specimen #28 surface

Table 13: elements concentration at specimen #28 surface from the EDS analysis.
Filter Fit, Chi² value: 4.254, Correct. Method: Proza (Phi-Rho-Z), Acc.Voltage: 20.0 kV, Take Off Angle: 90.0°.

Element	Weight conc. %	Atomic conc. %
Cr	6.4	6.9
Fe	93.6	93.1
W	-	-

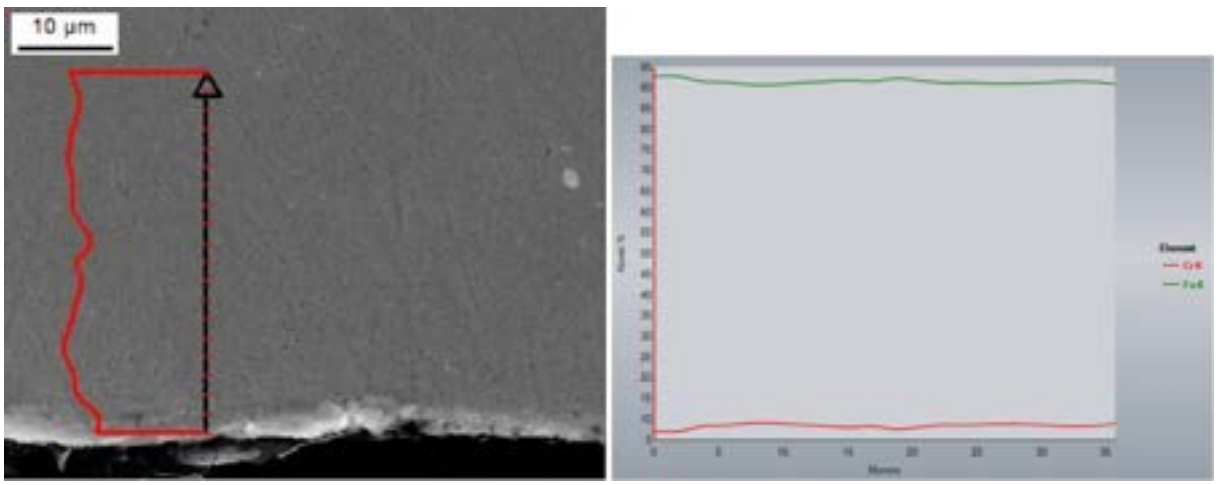

Figure 54: left: SEM image and Cr concentration profile (EDS) of specimen #28 section; right: Cr (red) and Fe (green) concentration profiles along the specimen section.

2.4.5.10 F82H: specimen #29 (4000 hours)

Last, but not least, specimen #29. Figure 55 shows, at magnitude 400X, a region of the external surface of this specimen. The general appearance of the surface is good, and characterized by the usual vertical stripes originated during the manifacturing of the sample. Anyway some localized alterations produced by corrosion phenomena are also visible, in the form of small pits and ulcerations; one of them, circled in red in Figure 55, can be better observed in the enlargement (4000X) riported in Figure 56.

On the surface of specimen #29 are present also a lot of dark spots, probably due to organic substance, as evidenced by Figure 57 (500X); moreover, when enlarging the centro-left/bottom of this figure to Figure 58 (4000X), in correspondance of these spots the surface seems also affected by a more pronounced degradation.

Figure 55: SEM image of specimen #29 surface (secondary electrons) at magnitude 400X. Scale bar above the image.

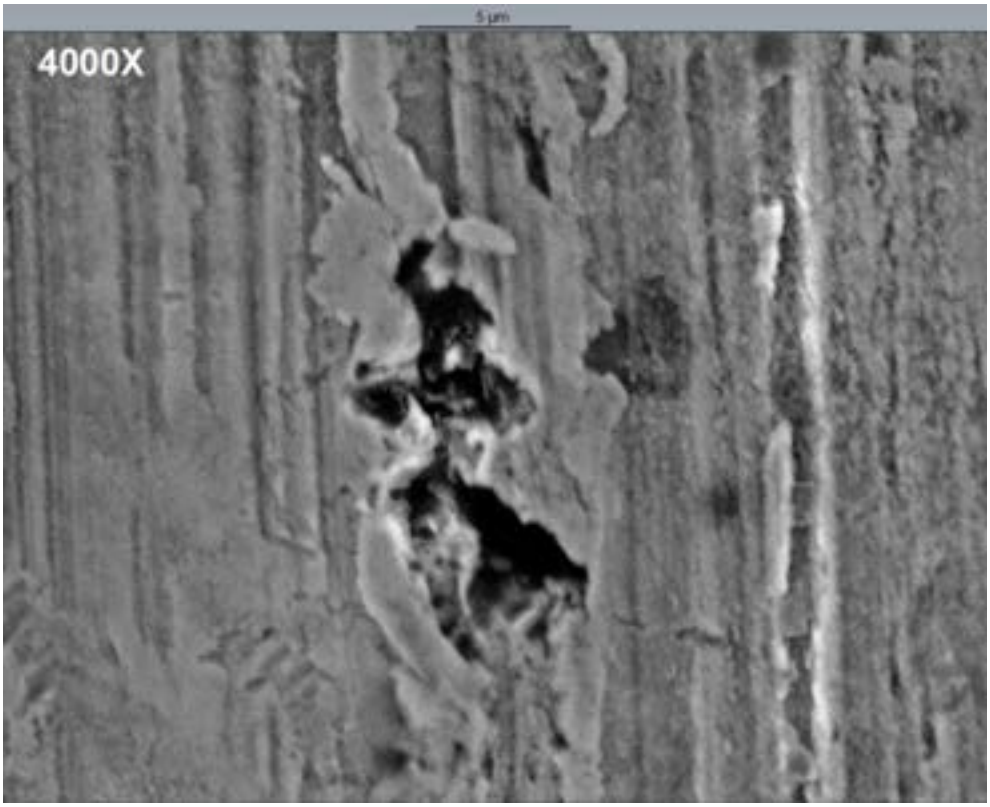

Figure 56: SEM image of specimen #29 surface (secondary electrons) at magnitude 4000X (enlargement of Figure 55). Scale bar above the image.

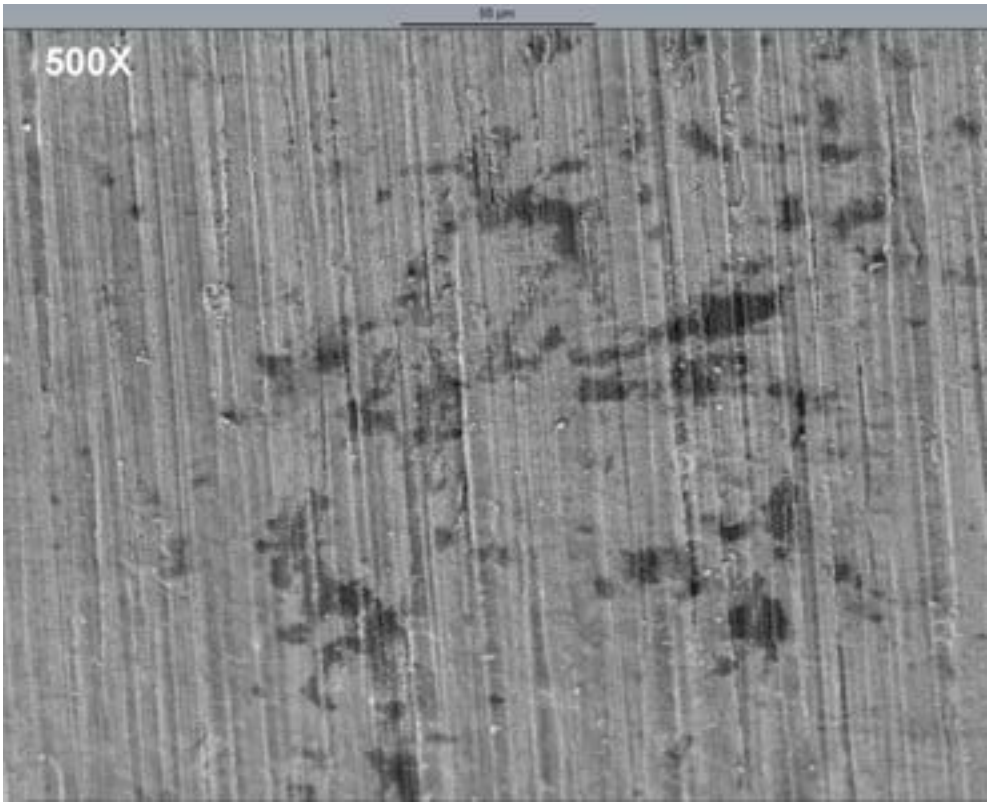

Figure 57: SEM image of an other portion of specimen #29 surface (secondary electrons) at magnitude 500X. Scale bar above the image.

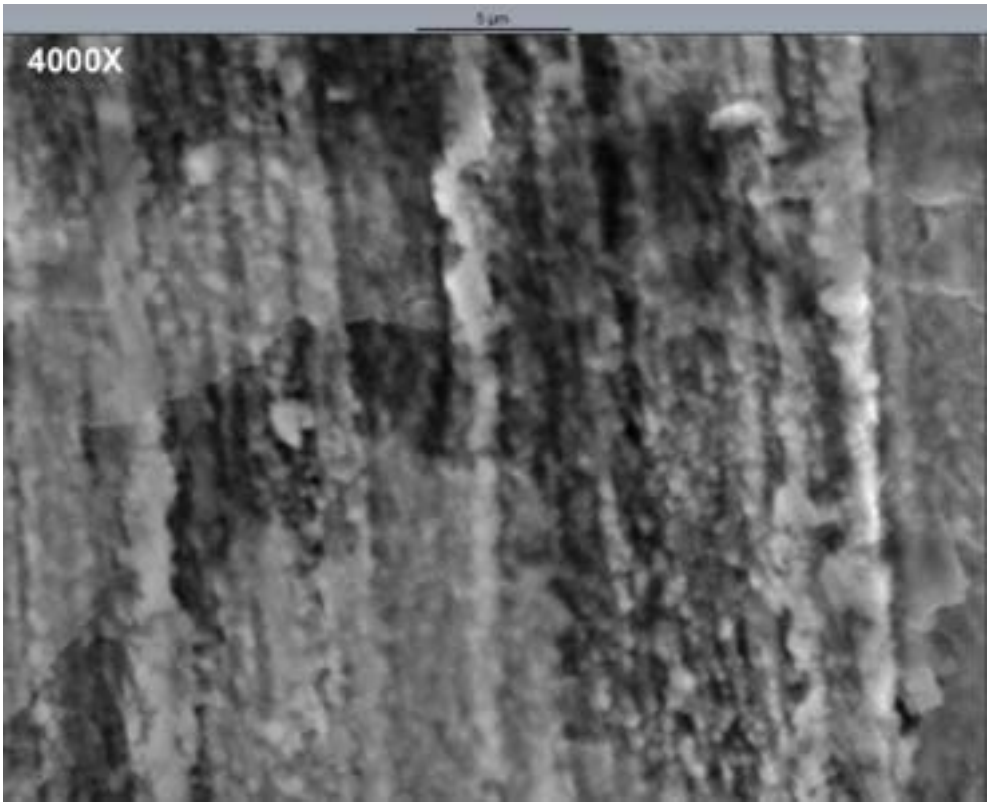

Figure 58: SEM image of specimen #29 surface (secondary electrons) at magnitude 4000X (enlargement of Figure 57). Scale bar above the image.

Figure 59 summarizes the EDS analysis outcome reporting the average spectrum of a large, intact, surface region; Table 14 converts it in weight % concentration numbers. The average chemical composition at the surface is very similar to the one measured for specimen #28 after the erosion-corrosion test (Table 10) and indicates a Chromium depletion equal to -1.6% by weight. Other elements are not found in a quantifiable amount. The rest of the analzyed material is then Iron.

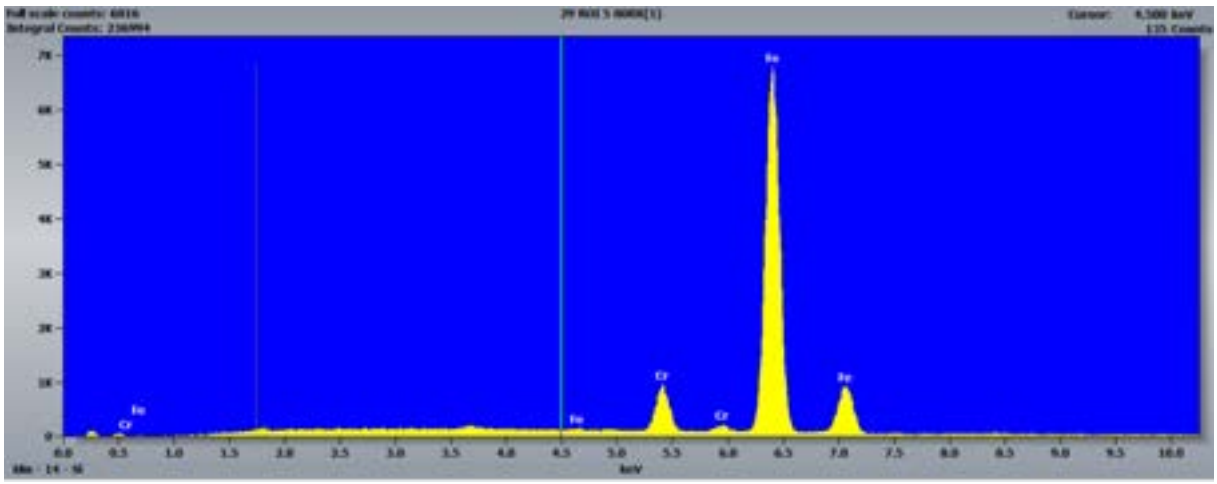

Figure 59: EDS spectrum obtained at specimen #29 surface

Table 14: elements concentration at specimen #29 surface from the EDS analysis.
Filter Fit, Chi² value: 4.254, Correct. Method: Proza (Phi-Rho-Z), Acc.Voltage: 20.0 kV, Take Off Angle: 90.0°.

Element	Weight conc. %	Atomic conc. %
Cr	6.3	6.7
Fe	93.7	93.3
W	-	-

Finally, Figure 60 (left) shows a SEM image at 2000X of a representative cross section of specimen #29, together with the overlapped Chromium concentration vs depth profile, constructed by the EDS analysis of equidistant points (~ 2 µm spaced), in the arrow direction. On the right side of Figure 60 is instead reported a graph showing the profiles of Chromium and Iron elements along the arrow direction, where y-axis is the atomic % concentration, while x-axis indicates the distance from the surface (the surface position is on the left boundary of the graph, in correspondence of x = 0). From the observation of Figure 60 left, it is possible to note that the internal specimen structure is in good condition, with no morphological alteration or grain detachment. The concentration profiles on the right indicate no increasing or decreasing trend of values moving inside the specimen. Small oscillations in Cr concentration are due to little local deviations from the theoretical alloy composition and/or to the analysis uncertainty; specular fluctuations are seen in Fe concentration values, since the sum of Cr and Fe makes always 100.

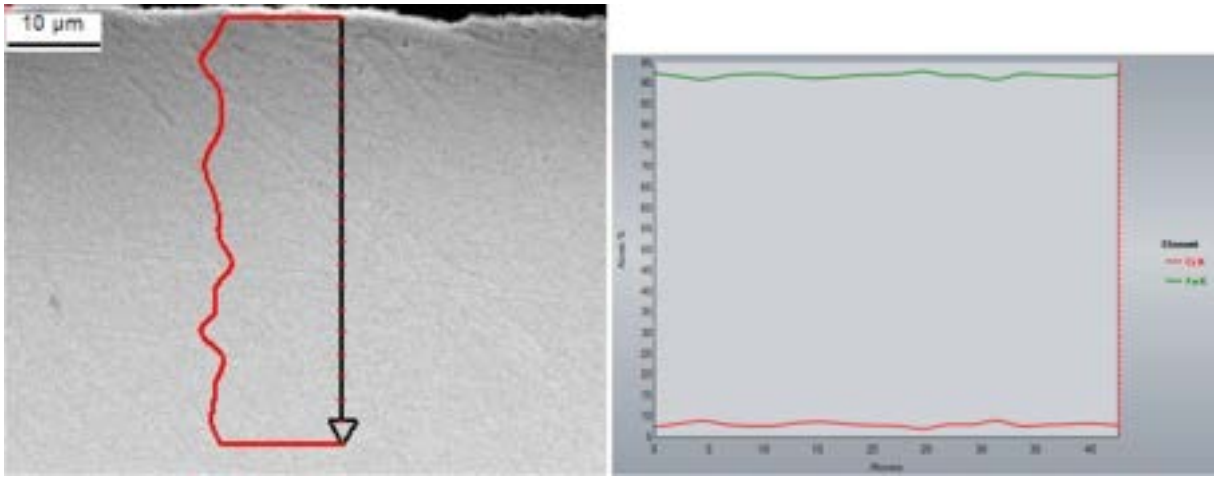

Figure 60: left: SEM image and Cr concentration profile (EDS) of specimen #29 section; right: Cr (red) and Fe (green) concentration profiles along the specimen section.

2.4.5.11 General considerations on the SEM-EDS analysis results

On the basis of the investigations reported in the previous subsections, it can be said that corrosion phenomena by flowing liquid Lithium occurred at a very low extent on the exposed specimens surfaces. The most evident objects, like parallel stripes and scratches and black spots, are in fact equally detected also on the surfaces of fresh unexposed specimens, being due respectively to the mechanical manufacturing of the specimens and to the presence of external contamination by organic substances, somehow occurred during the sample handling.

When analysing in detail the whole surface of each sample, some corrosion items can be additionally discovered, generally in the form of shallow pits with dimensions not exceeding ~ 10 µm, but their frequency is very low. From the SEM images reported in the previous subsections, the occurrence of these locally damaged areas seems to be slightly higher for F82H than for Eurofer 97, being them non reported at all for sample #12 (EU97), #7 (EU 97) and #32 (F82H), just suspected or minimal for sample #13 (EU97) and sample #8 (EU97), being instead more evident in samples #34 (F82H), #28 (F82H) and #29 (F82H, Figure 74). Anyway, being these alterations very few in absolute terms, this little difference between the 2 materials could fall within the statistical nature of the phenomenon, therefore it would be hard here to conclude that F82H was more susceptible to the aggressive action by Lithium.

A common evidenced feature of all the specimens is however a more 'granulose' appearance of the surfaces after the tests, which becomes more pronounced with the test duration. The surface irregularities originating this granulose aspect are submicrometric and not able to modify substantially the rugosity parameters (Ra, Rz, Rt), which, even for the 4000 hours specimens, result only a little decreased respect to the unexposed specimens (-5÷10% at most). This granulosity can be hence seen like a small noise imposed over the deeper preexisting grooves created at the moment of polishing the surface. Especially when looking at the longest test specimen (Figure 35), the surface would seem constituted of an array of very small stuck or dug corpuscles, whose formation could be associated with the observed depletion of Cr, according to the conclusion reported by Chopra [8] for the similar HT-9 alloy (but with ~12 wt.% of Cr and 0.6 wt.% of Ni) exposed to liquid (low speed) Li. Chopra dimples dimensions were larger than ours, anyway he tested its alloy at higher temperatures (372 to 538°C) and with a larger Nitrogen contamination, registering a larger Cr depletion at the surface (- 4÷6 wt.% in its samples); being our temperature lower, it is also possible that the development of our dimples is slower and increases therefore with the test time.

For what concerns the average elements concentrations measured by the EDS analysis at the surfaces of the specimens, they are summarized in Table 15.

Table 15: summary of elements concentrations at specimens surfaces from the EDS analysis (% by weight). Filter Fit, Chi² value: 4.254, Correct. Method: Proza (Phi-Rho-Z), Acc.Voltage: 20.0 kV, Take Off Angle: 90.0°.

Material	Eurofer 97	Eurofer 97	Eurofer 97	Eurofer 97	Eurofer 97	F82H	F82H	F82H	F82H	F82H
Sample ID	10	12	13	7	8	31	32	34	28	29
Cr	8.5	7.7	7.5	7.3	7.3	8.0	6.9	6.5	6.4	6.3
Mn	0.8	-	-	-	-	-	-	-	-	-
Fe	88.9	92.3	91.3	92.7	92.7	88.5	93.1	93.5	93.6	93.7
W	1.8	-	1.2	-	-	3.5	-	-	-	
ΔCr	***Unexposed***	**-0.8**	**-1.0**	**-1.2**	**-1.2**	***Unexposed***	**-1.1**	**-1.5**	**-1.6**	**1.7**
ΔW	***Unexposed***	**-1.8**	**-0.6**	**-1.8**	**-1.8**	***Unexposed***	**-3.5**	**-3.5**	**-3.5**	**-3.5**
		2000 hours		**4000 hours**			**2000 hours**		**4000 hours**	

Even if the EDS analysis is intrinsically affected by a 0.5% uncertainty in the atomic element composition, when comparing the exposed with the fresh specimens values the Chromium concentration decrease at the surface is evident, as already verified during the previous erosion-corrosion tests [3]. It would also seem, on the average, that this depletion is slightly more pronounced for specimens exposed to Lithium for 4000 hours, i.e. the ones already exposed to 2000 hours during the mid-term test and then exposed again to 2000 hours in this test. On the whole, a slighlty higher Chromium depletion of F82H (average: -1.5%) respect to Eurofer 97 (average: -1.05%) can also be seen.

Similarly, also the Manganese (for Eurofer 97) and Tungsten depletion is evident. For both the tested materials, the residual Tungsten concentration after the test is generally close to 0, which would indicate a larger (in absolute terms) decrease for F82H material, characterized by a greater starting concentration of this metal. Actually, a small difference can be seen between the 2000 and the 4000 hours specimens. While for the first ones some residual traces of Tungsten peaks can be seen in the related EDS spectra (corresponding anyway to amounts below the quantification limit), for the longest exposure ones the peaks are effectively more difficult to distinguish or are completely absent: the double time contact with liquid Lithum did produce a more complete Tungsten removal at the surface.

Finally, it must be observed that the inner structure (down to about 40-45 µm) of all the exposed samples was not affected by the action of flowing Lithium, as revealed by the SEM analysis of the specimens sections. Moreover, the Chromium concentration vs depth profiles were all rather flat, with only small fluctuations due to random local non homogeneities of the alloy or to the uncertainty of the analysis.

3 Conclusioni

Both Eurofer 97 and F82H exhibited a good resistance behavior to the experimental test conditions.

The maximum registered corrosion rate of all the specimens was about 0.29 µm/y, a value largely lower than the limit set for the IFMIF Target backwall (1 µm/y), and around 1 order of magnitude lower than in the previous experiment performed with LIFUS 3 plant [2]. Since in that test the precise value of Nitrogen concentration in Lithium was unknown, but supposed to be of the order of some hundredths of wppm, while in this test it has been verified as always ≤ 30 wppm, and since all the other parameters are essentially identical, it is reasonable to ascribe to the higher purity of Lithium the good result of this test. Speaking of which, it must in fact be remembered also the outcome of Chopra and Smith experimentation [8], who noticed, for a similar ferritic-martensic steel (HT-9), how the corrosion rate increased by about 1 order of magnitude increasing the Nitrogen concentration from ~ 50 to ~ 250 wppm.

Very few and small corrosion items were detected on the exposed surfaces; the arise of a granulose appearance was evidenced, especially after longer exposure times.

A little Cr and W decrease was measured in the average surface compositions; difference between the 2 materials were trivial, with a higher Cr depletion from F82H surfaces, but so small to fall within the measurement uncertainty. The Cr depletion can be rationalized according to the formation of Li_9CrN_5 [9].

The internal structure of all the specimens was no way damaged: a small inhomogeneity could be actually present in a submicron (or 1-2 microns, at most) layer below the exposed surface, but to characterize a so thin layer some additional and more specific technique would be necessary.

The study of the steels resistance to the erosion-corrosion exerted by flowing Lithium has not been concluded with the test detailed in this report. In a close future experimentation, Lifus 6 plant will be employed again for this activity, allowing test durations longer than 4000 hours. Additionally, parametric studies will be performed, in which the concentration of Nitrogen in Lithium will be progressively raised till hundreds of wppm, to better quantify the effect of this parameter on the corrosion rate and in case

highlight the existance of a threshold, above which the behaviour of the exposed steels becomes all at once worse.

4 Riferimenti bibliografici

1. IFMIF International Team “IFMIF Comprehensive Design Report”, 2004
2. P. Agostini “Corrosion/erosion of steels in Lithium: LIFUS3 tests”, Enea Report IM-A-R-004, 25/2/2008
3. P. Favuzza, M. Cuzzani, G. Fasano “Risultati relativi alle campagne sperimentali di breve e medio termine sui fenomeni di erosione/corrosione da litio liquido fluente nell’impianto Lifus 6”, Report Rds/PAR2015, Settembre 2016
4. A. Aiello, M. Cuzzani, G. Fasano, P. Favuzza, R. Giammusso, M. Granieri, S. Mannori, M. Muzzarelli, F.S. Nitti, L. Sansone, M. Tarantino, A. Tincani “Test Definition Report”, IFMIF/EVEDA Deliverable LF 3.1, October 2016
5. P. Favuzza “Delivery of F82H and Eurofer Steel for Test of Specimens”, IFMIF/EVEDATechnical Note LF3 NP-1, March 2013
6. P. Favuzza, S. Mannori “Acceptance Test Report of the Lifus 6 Purification System”, IFMIF/EVEDA Deliverable LF 4.4.3, May 2015
7. P. Favuzza et al. “Round Robin test for the determination of nitrogen concentration in solid Lithium”, Fus. Eng. Des. 107 (2016) 13-24
8. O.K. Chopra and D.L. Smith “Influence of temperature and lithium purity on corrosion of ferrous alloys in flowing lithium environment”, J. Nucl. Mater. 141&143 (1986), 584-591
9. V.P. Krasin and S.I. Soyustova, Thermodynamic analysis of chromium solubility data in liquid lithium containing nitrogen: comparison between experimental data and computer simulation, J. Nucl. Mater. 465 (2015) 674-681

5 Abbreviazioni ed acronimi

EDS	Energy Dispersive X-ray Spectrometry
EVEDA	Engineering Validation and Engineering Design Activities
IFMIF	International Fusion Materials Irradiation Facility
wppm	Weight Parts per Million
Ra, Rt, Rz	Rugosity Parameters
RAFM	Reduced Activation Ferritic Martensitic
SEM	Scanning Electron Microscopy